Dutova, E. M., Nikitenkov, A. N., Pokrovskiy, V. D., Banks, D., Frengstad, B. S. and Parnachev, V. P. (2017) Modelling of the dissolution and reprecipitation of uranium under oxidising conditions in the zone of shallow groundwater circulation. *Journal of Environmental Radioactivity*, 178-17, pp. 63-76.

This the final accepted version of this article, available under a Creative Commons License: https://creativecommons.org/licenses/by-nc-nd/4.0/.

The published version is available : https://doi.org/10.1016/j.jenvrad.2017.07.016

http://eprints.gla.ac.uk/146083/

Deposited on: 24 August 2017

Enlighten – Research publications by members of the University of Glasgow
http://eprints.gla.ac.uk

Modelling of the dissolution and reprecipitation of uranium under oxidising conditions in the zone of shallow groundwater circulation

Ekaterina M. Dutova[1], Aleksei N. Nikitenkov[2], Vitaly D. Pokrovskiy[3], David Banks[4,5], Bjørn S. Frengstad[6] and Valerii P. Parnachev[7]

[1,2,3] Tomsk Polytechnic University, Prospekt Lenina 30, 634050 Tomsk, Russia

[4] School of Engineering, James Watt Building (South), University of Glasgow, Glasgow, G12 8QQ, United Kingdom

[5] Holymoor Consultancy Ltd., 360 Ashgate Road, Chesterfield, S40 4BW, United Kingdom

[6] Department of Geoscience and Petroleum, Norwegian University of Science and Technology, NO-7491 Trondheim, Norway

[7] Department of Dynamic Geology, Faculty of Geology and Geography, Tomsk State University, Prospekt Lenina 36, 634050 Tomsk, Russia.

E-mail: [1]dutova@sibmail.com, [2]corestone@mail.ru, [3]pokrovskiy.v@gmail.com, [4,5]david.banks@glasgow.ac.uk, [6]bsfrengstad@yahoo.no, [7]dingeo@ggf.tsu.ru

Abstract. Generic hydrochemical modelling of a grantoid-groundwater system, using the Russian software "HydroGeo", has been carried out with an emphasis on simulating the accumulation of uranium in the aqueous phase. The baseline model run simulates shallow granitoid aquifers (U content 5 ppm) under conditions broadly representative of southern Norway and southwestern Siberia: i.e. temperature 10°C, equilibrated with a soil gas partial CO_2 pressure (P_{CO2}, open system) of $10^{-2.5}$ atm. and a mildly oxidising redox environment (Eh = +50 mV). Modelling indicates that aqueous uranium accumulates in parallel with total dissolved solids (or groundwater mineralisation *M* – regarded as an indicator of degree of hydrochemical evolution), accumulating most rapidly when *M* = 550 – 1000 mg L^{-1}. Accumulation slows at the onset of saturation and precipitation of secondary uranium minerals at *M* = c. 1000 mg L^{-1} (which, under baseline modelling conditions, also corresponds approximately to calcite saturation and transition to Na-HCO_3 hydrofacies). The secondary minerals are typically "black" uranium oxides of mixed oxidation state (e.g. U_3O_7 and U_4O_9). For rock U content of 5 to 50 ppm, it is possible to generate a wide variety of aqueous uranium concentrations, up to a maximum of just over 1 mg L^{-1}, but with typical concentrations of up to 10 µg L^{-1} for modest degrees of hydrochemical maturity (as indicated by *M*). These observations correspond extremely well with real groundwater analyses from the Altai-Sayan region of Russia and Norwegian crystalline bedrock aquifers. The timing (with respect to *M*) and degree of aqueous uranium accumulation are also sensitive to Eh (greater mobilisation at higher Eh), uranium content of rocks (aqueous concentration increases as rock content increases) and P_{CO2} (low P_{CO2} favours higher pH, rapid accumulation of aqueous U and earlier saturation with respect to uranium minerals).

Keywords: Natural uranium, groundwater, mineralisation, ore, solubility, hydrochemical modelling

Highlights:

- The computer model "HydroGeo" has been credibly applied to dissolution of uranium from silicate rocks.
- Uranium solubility in shallow groundwaters is limited by precipitation of mixed hexavalent-tetravalent uranium oxides.
- As redox potential and host-rock uranium concentrations increase, aqueous uranium concentrations also generally increase.
- Aqueous U concentrations of up to 10 µg L^{-1} are typical for shallow granite groundwaters, with up to 1 mg L^{-1} being simulated in the most evolved waters.
- Field studies of uranium in groundwater in Norway and Southern Siberia broadly support the modelling findings.

1. Introduction

The occurrence of natural uranium in surface- and groundwaters has obvious importance for human health and drinking water policy (Reimann & Banks 2004, WHO 2012, Frengstad & Banks 2014); moreover, it has implications for ore formation and prospecting. The mechanisms of uranium accumulation in the aqueous phase and its behaviour in natural waters are topics that have occupied many scientists (Lisitsin 1971, Grenthe *et al.* 1992, Kislyakov & Shchetochkin 2000, Barnett *et al.* 2000, Runde 2000, Bain *et al.* 2001, Kondratyeva & Nesterova 2002, Barsukov & Borisov 2003, Krainov *et al.* 2004, Shvartsev *et al.* 2007, Dutova & Nikitenkov 2010, Frengstad & Banks 2008, 2014, Ariunbileg 2016). It is broadly recognised that, while uranium forms a variety of uranium (+VI) oxy-ions and complex ions that permit its accumulation and mobilisation in relatively high concentrations in oxidising aqueous environments, its behaviour is redox-sensitive. The mobility of uranium in reducing environments can be severely limited, at least at circum-neutral pH, by the formation of reduced (uranium (+IV)) secondary minerals. This is also the reason why primary uranium deposits tend to be formed in redox-front (e.g. "roll-front") environment (such uranium deposits formed by precipitation from aqueous solution are typically termed "hydrogene" in Russian terminology). Although laboratory and field studies have allowed a generally good understanding of the occurrence and behaviour of aqueous uranium, some uncertainties remain. Does uranium (+VI) reach concentrations which represent an "equilibrium" with a given mineral assemblage? To what extent can it continue to accumulate in the aqueous phase before reaching a mineral saturation "ceiling"? Do observed high concentrations (e.g. in the mg L^{-1} range: Frengstad *et al.* 2000, Frengstad & Banks 2014) represent some form of supersaturated state, with mineral precipitation limited only by kinetic constraints?

This paper represents a continuation of the research carried out by the Tomsk research team (Bukaty *et al.* 2010, Dutova & Nikitenkov 2010) and focuses on the behaviour of uranium in oxidising conditions in the zone of shallow groundwater circulation (often referred to in Russian literature as the "hypergene" zone). Such conditions are, of course, widely encountered by hydrogeologists and geochemists, not least in the context of uranium toxicity in potable groundwater (Frengstad & Banks 2014). In a Russian context, we consider especially groundwater discharge areas adjacent to the folded, metamorphic and igneous cores of orogenic belts - regarded as being favourable for the accumulation of hydrogene uranium deposits

(Kondratyeva *et al.* 1980). The methods used for the physico-chemical modelling of uranium in this paper have been selected to best reflect the natural conditions, pH and redox ranges encountered in Russian field studies (Lisitsin 1996, Barsukov & Borisov 2003, Bukaty 2005a, Shvartsev *et al.* 2007, Bukaty *et al.* 2010, Chudnenko 2010).

2. Software and Methods

2.1 The HydroGeo Code

The software package "HydroGeo", developed by M.B. Bukaty, has been selected as the preferred modelling tool for the study of uranium hydrochemistry reported here (Bukaty 2002, 2005a, 2005b, 2008). HydroGeo, like many other similar models developed in western Europe or the USA (such as MINTEQA or PHREEQC; Allison *et al*. 1991, Parkhurst & Appelo 1999), models the thermodynamic processes of dissolution and precipitation, solving for minimisation of free energy. Like other models, it relies upon a comprehensive database of thermodynamic data for minerals and reactions. Unlike the standard versions of some other modelling tools, however, it does have access to databases which include data on the thermodynamic properties of uranium minerals and species, culled from various sources including cprons92, SUPCRT (Helgeson *et al.* 1978, Johnson *et al.* 1992, Arthur 2001, Anderson 2009), UNITHERM (Shvarov & Bastrakov 1999, Cleverley & Bastrakov 2005), Berman (1988), and the NAGRA NTB report series.

For readers unfamiliar with this type of hydrogeochemical modelling, such models essentially start with a set of initial components (mineral assemblage, water and CO_2). These components are allowed to react with each other by solving a large set of simultaneous equations, each equation representing the thermodynamic equilibrium between two (or occasionally more) species. Constraints can be imposed on certain reactions (kinetic constraints, or specification of which minerals are allowed to precipitate when they become supersaturated), but the model ultimately seeks the solution to the large set of simultaneous equations within these constraints. The model keeps internal account of all dissolved species (such as protons, dissolved CO_2, redox-sensitive species or uranyl species, such as UO_2OH^+), such that pH, Eh, total dissolved solutes (mineralisation) or total dissolved uranium can be calculated at any stage of the simulated hydrochemical evolution. The detail of such modelling is beyond the scope of this

paper, but the interested reader is referred to Kharaka *et al.* (1988), Allison *et al*. (1991), Parkhurst & Appelo (1999), Ball & Nordstrom (2001), Alekseev *et al.* (2005) and Bukaty (2002, 2005a, 2005b).

The HydroGeo model has been extensively tested against comparable international models, including the HMV model (Harvie *et al.* 1984, Bukaty 2005b). The use of the software HydroGeo for solving various problems has demonstrated earlier by Shvartzev & Dutova (2001), Dutova *et al.* (2006), Gaskova *et al.* (2009), Dutova & Nikitenkov (2010), Dutova *et al.* (2016) and Balobanenko *et al.* (2016).

2.2. Defining the Modelled Problem

In this study, the model considered the interaction of groundwater with granitoids under conditions characteristic of the zone of shallow groundwater circulation (temperature = 10°C, pressure = 1 MPa, equivalent to 100 m hydraulic head or 10 bars). The uranium content of the rocks, assumed to be present within the primary mineral phases, was set at between 5 ppm and 500 ppm. The environment was simulated as mildly oxidising, with an initial Eh of between +5 to +100 mV (although the Eh was allowed to vary as the reaction progresses). The model assumes a system which is open with respect to CO_2, equilibrated with various putative soil gas partial pressures ($P_{CO2} = 10^{-0.5}$, $10^{-1.5}$, $10^{-2.5}$ atm.). Henceforth in this paper, the term "partial pressure" will refer to the (soil) gas-phase partial pressure with which the water is equilibrated. This situation is believed to be characteristic for groundwater drainage from granitoid-containing hydrogeological massifs. Naturally, the higher the P_{CO2}, the lower the initial water pH.

The composition of the simulated granitoid mineral assemblage was broadly based on the composition of granitoids that are common in mountainous areas of southwestern Siberia (Western and Eastern Sayan mountains, Kuznetsk Alatau, Altai, Salair and the Kolyvan'-Tomsk folded zone - Babin *et al.* 2007, Banks *et al.* 2008, 2011, Korobeinikov *et al.* 1983, Voroshilov *et al.* 2014). These are predominantly Cambro-Ordovician granitoids intruded into a Precambrian-Cambrian suite of metavolcanics and metasediments. Specifically, the modelling assumed an assemblage comprising 60% plagioclase ($An_{30}Ab_{70}$), 23% quartz, 5% hornblende, 7% biotite and 5% potassium feldspar. Calcite is initially assumed to be absent.

The parent mineral assemblage is indicated in Table 1. The uranium was introduced in the model in its hexavalent form as a substitute for Ca and Al proportionately in the matrices of all of the aluminosilicate mineral phases (except quartz) listed in Table 1. Accordingly, uranium is released to the water phase as the minerals are hydrolysed.

The rate of dissolution / hydrolysis of the various mineral phases is calculated on the basis of initial reaction / dissolution rate constants, relative to a reference reaction. As reaction products accumulate in the aqueous phase and equilibrium is approached, the net rates of reaction decrease according to the relevant rate laws. Precipitation, once saturation has been achieved with respect to the secondary minerals, is assumed to be instantaneous. Sorption is not explicitly included in these simulations.

163

164 **Table 1. Parent mineral phases included in the model**

	Name	Formula	% volume of the rock
1	Pargasite (hornblende)	$Na(Ca)_2(Fe^{II})_4Al_3Si_6O_{22}(OH)_2$	5
2	Pargasite (hornblende)	$Na(Ca)_2Mg_4Al_3Si_6O_{22}(OH)_2$	
3	Albite	$Na(Al)Si_3O_8$	42
4	Anorthite	$(Ca)Al_2Si_2O_8$	18
5	Quartz	SiO_2	23
6	Potassium feldspar	$K(Al)Si_3O_8$	5
7	(K-Fe^{II}) biotite	$K(Fe^{II})_3(Al)Si_3O_{10}(OH)_2$	7
8	(Na-Fe^{II}) biotite	$Na(Fe^{II})_3(Al)Si_3O_{10}(OH)_2$	

165

166 **Table 2. A listing of the secondary minerals considered in the modelling of the**
167 **groundwater-granitoid geochemical system.**

Mineral no.	Name	Formula
Carbonates		
1	Calcite	$CaCO_3$
2	Aragonite	$CaCO_3$
3	Dolomite	$CaMg(CO_3)_2$
4	Siderite	$Fe^{II}CO_3$
Oxides / hydroxides		
5	Goethite	$Fe^{III}OOH$
6	Hematite	$Fe^{III}{}_2O_3$
7	Gibbsite	$Al(OH)_3$
Silicates		
8	Amorphous silica	SiO_2
9	Chalcedony	SiO_2
10	Mg-serpentine (chrysotile)	$Mg_6Si_4O_{10}(OH)_8$
Aluminosilicates		
11	Kaolinite	$Al_2Si_2O_5(OH)_4$
12	Ca-Montmorillonite	$Ca_{0.15}Al_{1.9}Si_4O_{10}(OH)_2$
13	K-Montmorillonite	$K_{0.3}Al_{1.9}Si_4O_{10}(OH)_2$
14	Mg-Montmorillonite	$MgAl_2Si_4O_{11}(OH)_2$
15	K-Fe^{III} illite	$K_{0.5}(Fe^{III})Al_{1.5}Si_{3.5}O_{10}(OH)_2$
16	Muscovite	$KAl_3Si_3O_{10}(OH)_2$
17	Mg-beidellite	$Mg_{0.165}Al_{2.33}Si_{3.67}O_{10}(OH)_2$
18	Mg-chlorite	$Mg_{4.5}Al_3Si_{2.5}O_{10}(OH)_8$
Uranium minerals		
19	Amorphous UO_2	UO_2
20	Uraninite	UO_2
21	Schoepite	$UO_2(OH)_2(H_2O)$
22	Rutherfordine	UO_2CO_3
23	$(UO_3)(UO_2)_2$ (“black” oxide) alpha	α-U_3O_7
24	$(UO_3)_2(UO_2)$ (“black” oxide)	U_3O_8
25	$(UO_3)(UO_2)_2$ (“black” oxide) beta	β-U_3O_7
26	$(UO_3)(UO_2)_3$ (“black” oxide)	U_4O_9
27	α-$(UO_2)O$	UO_3
28	β-UO_3	UO_3
29	γ-UO_3	UO_3
30	β-schoepite	$UO_2(OH)_2(H_2O)$
31	Soddyite	$(UO_2)_2SiO_4(H_2O)_2$
32	Amorphous coffinite	$USiO_4$
33	Coffinite	$USiO_4$

168

169 The modelling of the aqueous phase considered redox potential and the following main ionic
170 components (and their aqueous complex ions): H^+ / OH^-, Na^+, K^+, Ca^{2+}, Mg^{2+}, Fe^{2+} / Fe^{3+}, Al^{3+},
171 SO_4^{2-}, Cl^-. The following uranium species were also considered within the model: $(UO_2)^{2+}$, U^{4+},
172 $(UO_2HCO_3)^+$, $UO_2(HCO_3)_2$, UO_2CO_3, $(UO_2(CO_3)_2)^{2-}$, $(UO_2(CO_3)_3)^{4-}$, $(UO_2(CO_3)_3)^{5-}$,

$((UO_2)_2CO_3(OH)_3)^-$, $(U(CO_3)_4)^{4-}$, $(U(CO_3)_5)^{6-}$, UO_2SO_4, $(UO_2(SO_4)_2)^{2-}$, $UO_2(HSO_4)_2$, $(UO_2HSO_4)^+$, $(USO_4)^{2+}$, $U(SO_4)_2$, UO_2Cl^+, $(UCl)^{3+}$, $(UCl_2)^{2+}$, $(UO_2)^+$, $(UOH)^{3+}$, $(U(OH)_2)^{2+}$, $U(OH)_4$, $(U(OH)_3)^+$, $((UO_2)_3(OH)_4)^{2+}$, $(UO_2(OH)_4)^{2-}$, $(UO_2(OH)_3)^-$, $((UO_2)_2(OH))^{3+}$, $((UO_2)_3(OH)_7)^-$, $((UO_2)_3(OH)_5)^+$, $((UO_2)_2(OH)_2)^{2+}$, $UO_2(OH)_2$, UO_2OH^+, $((UO_2)_4(OH)_7)^+$, UO_2OH, $(HUO_3)^-$, $(HUO_4)^-$, $(UO_4)^{2-}$, $(UOH)^{2+}$, $(UO_3)^-$, $(HUO_2)^+$.

The modelling also considered 33 secondary solid phase minerals, of which 15 were uranium-containing (Table 2). Metal-uranyl complexes (e.g. Ca-uranyl complexes, which can be important in defining the aqueous behaviour of uranium; Dong & Brooks 2006, Stewart 2008, Lietsch *et al.* 2014) were not explicitly included in the simulations, both for reasons of simplicity and because the cationic composition of the system may be rather lithology-dependent.

The evolved water composition was, at each step of the modelling process, reacted with the rock mineral assemblage derived from the previous step of modelling. The results are presented as a series of graphs, showing the evolution of the composition of the aqueous and solid phase with each step of the modelling process. The correspondence of the modelling results to real world hydrogeochemistry was "reality-checked" by comparison with real secondary mineralogical assemblages, absolute concentrations of parameters in groundwaters and ratios of elements in groundwaters (Shvartsev & Dutova 2001, Dutova *et al.* 2006).

3. Results

3.1 Modelling results: baseline case

Figures 1 to 4 show the evolution of the composition of the aqueous phase and the secondary mineral assemblage, focussing on the distribution of uranium at 10°C, total pressure of 1 MPa, a soil gas carbon dioxide partial pressure (P_{CO2}, with which the water is equilibrated) of $10^{-2.5}$ atmospheres and an initial Eh of +50 mV. In each case, the initial rock uranium content was 5 ppm. The degree of hydrochemical evolution is indicated by plotting against total water mineralisation (i.e. total dissolved solids) in the range 0 to 1500 mg L^{-1} on the y-axis.

The modelled evolution of the water is characterised, at all stages, by a progressive rise in pH from mildly acidic (containing dissolved CO_2) to mildly alkaline (Figure 1). The greatest changes in the chemical composition of the water are related to the removal of certain elements by precipitation within secondary mineral phases. Especially marked are the changes in concentration of calcium and magnesium in solution, related to the formation of carbonate (and other) minerals.

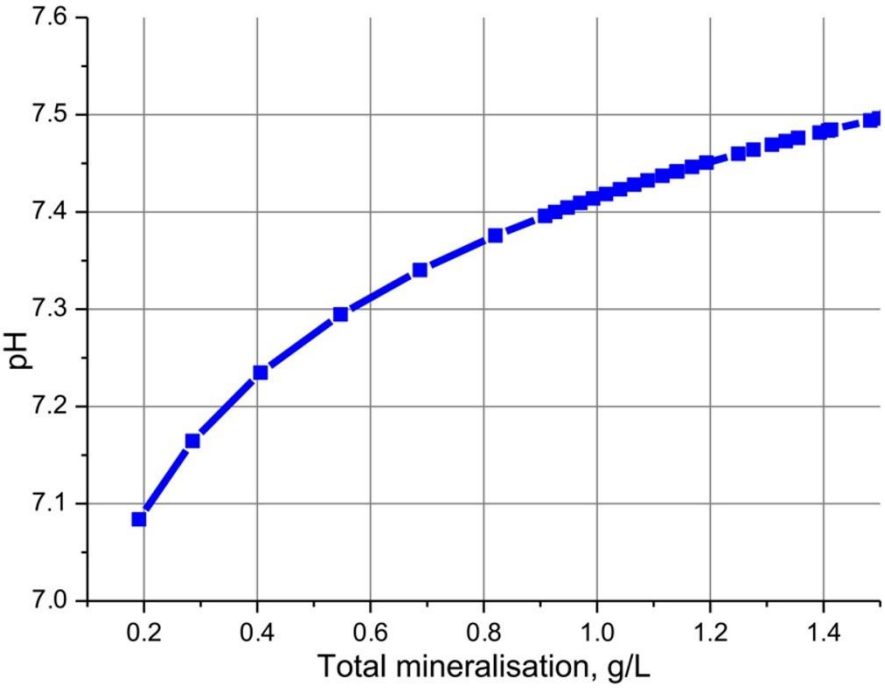

Figure 1. The evolution of the pH of the aqueous phase simulated in the groundwater-granitoid system, as a function of total mineralization (temperature = 10°C, P_{tot} =1 MPa, P_{CO2} = $10^{-2.5}$ atm., Eh = +50 mV, initial uranium content in rocks = 5 ppm)

This behaviour contrasts with that of sodium which, lacking significant insoluble secondary mineral phases, continues to accumulate in the water throughout the evolution of the simulation (Figure 2). In the early stages of modelled evolution, a calcium-sodium bicarbonate type of water is formed. At a total mineralisation (M) of around 550 mg L^{-1}, the soluble calcium content is depleted due to carbonate (calcite) precipitation and the continued accumulation of sodium leads to sodium-(calcium)-bicarbonate waters, as also observed by Banks & Frengstad (2006) and Frengstad & Banks (2007). The final phase of the simulated evolution of the system occurs at a mineralisation of around 900 mg L^{-1}, when magnesium begins to be removed from solution.

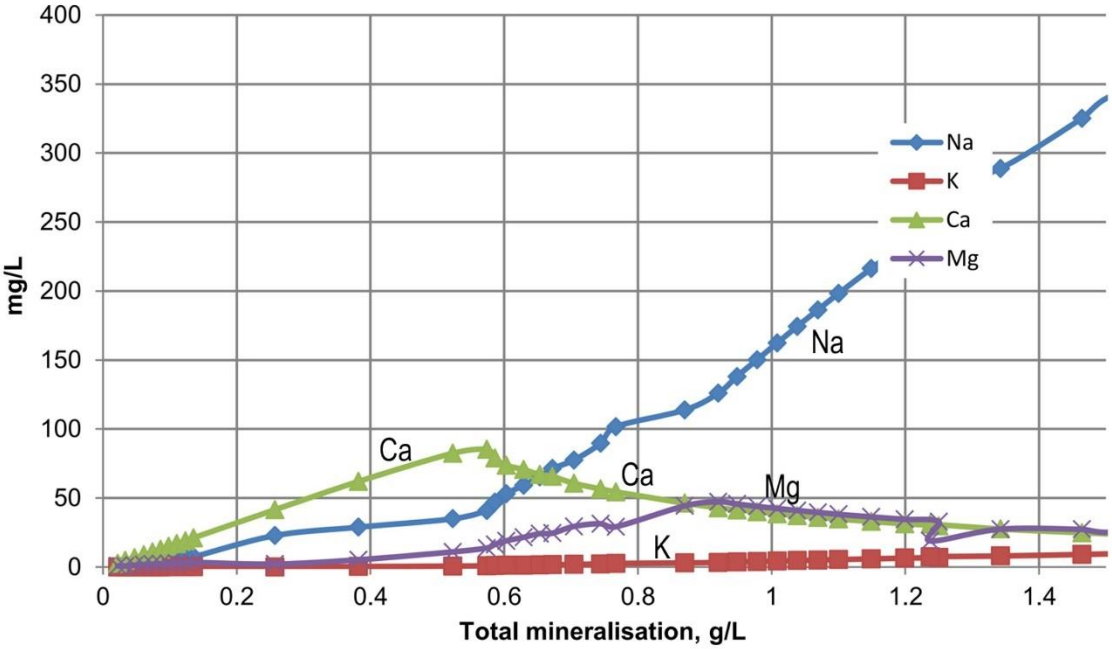

Figure 2. The evolution of the cationic composition of the aqueous phase simulated in the groundwater-granitoid system, as a function of total water mineralisation (temperature = 10°C, P_{tot} =1 MPa, P_{CO2} = $10^{-2.5}$ atm., Eh = +50 mV, initial uranium content in rocks = 5 ppm)

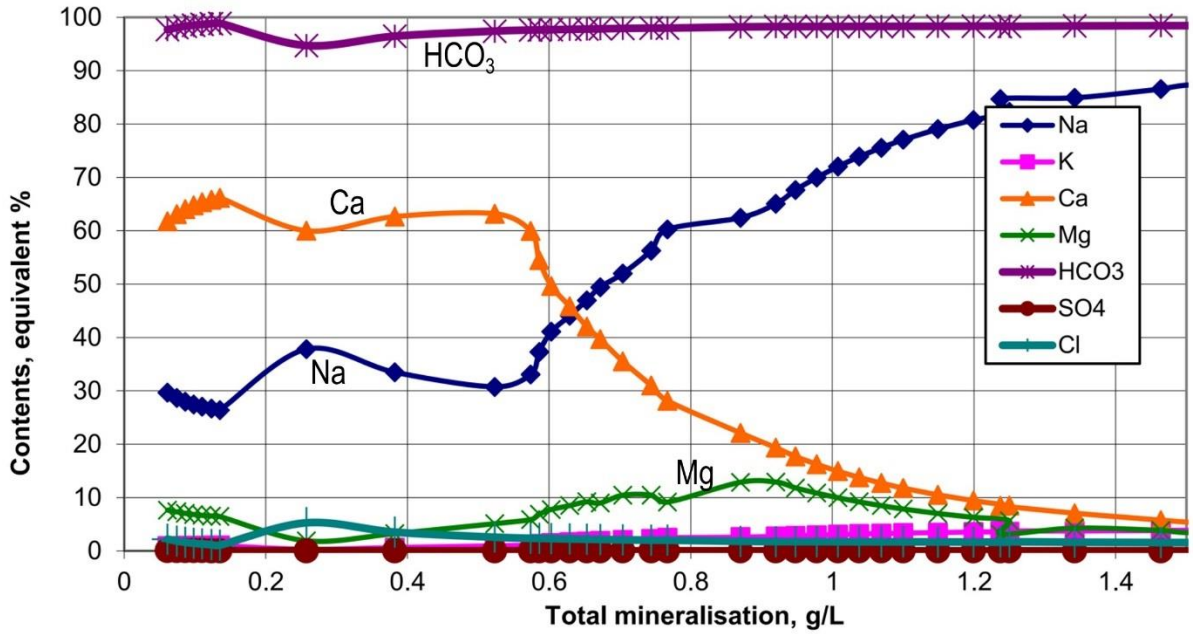

Figure 3. The evolution of the major ion composition of the aqueous phase simulated in the groundwater-granitoid system, as a function of total water mineralisation (temperature = 10°C, P_{tot} =1 MPa, P_{CO2} = $10^{-2.5}$ atm., Eh = +50 mV, initial uranium content in rocks = 5 ppm). Ions are shown as the ionic equivalent percentage of the total cations or anions, respectively, in solution.

All changes in the chemistry of the aqueous phase are reflected in corresponding changes in the secondary (solid phase) mineral assemblage. Thus, the depletion of calcium in the aqueous phase at M = 550 mg L^{-1} is related to the precipitation of calcite (Figure 4). The greatest intensity of secondary carbonate precipitation occurs in the interval M = 550-650 mg L^{-1}, preceding the formation of a sodium-bicarbonate type groundwater. As the groundwater becomes dominated by sodium as the major cation, the intensity of calcium depletion decreases dramatically. Similarly, at M = 900 mg L^{-1}, the depletion of magnesium from the aqueous phase corresponds to the progressive accumulation of secondary magnesium minerals (Figure 2) such as montmorillonite, Mg-illite and dolomite. At early stages of evolution montmorillonite is the dominant secondary Mg mineral, although as sodic water becomes dominant, magnesium is primarily removed from solution as dolomite.

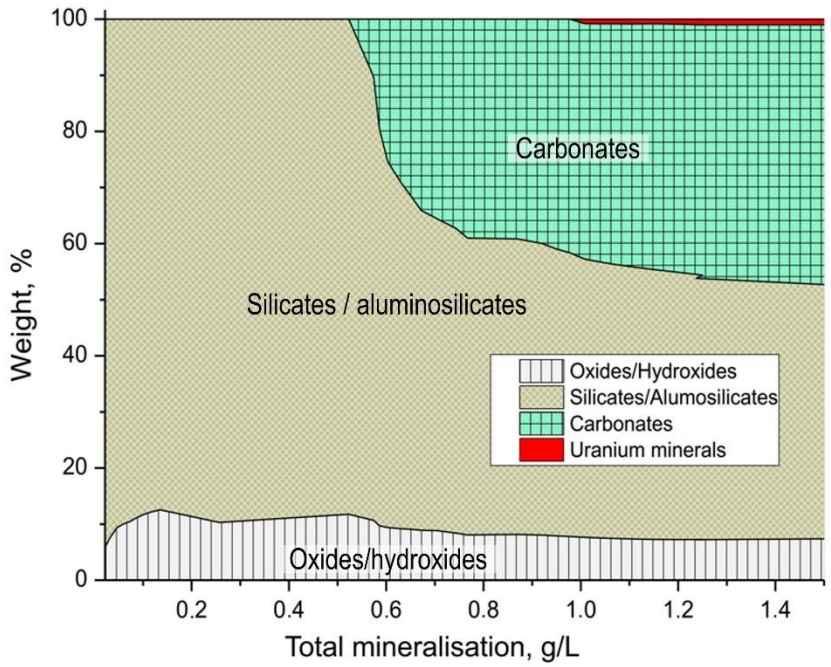

Figure 4. The mass fraction distribution of secondary minerals (as a proportion of the total mass of secondary minerals), as a function of total groundwater mineralisation in the simulated groundwater-granitoid system (temperature = 10°C, P_{tot} =1 MPa, $P_{CO2} = 10^{-2.5}$ atm., Eh = +50 mV, initial uranium content in rocks = 5 ppm).

The accumulation of dissolved uranium in the groundwater of the simulated water-granitoid system is quite complex (Figure 5). The rate of accumulation of uranium, as a function of mineralisation ($\Delta U/\Delta M$, in µg per 100 mg mineralisation M) abruptly increases from 0.2 µg per 100 mg in the range M = 0 to 550 mg L^{-1} (the domain of calcium-sodium-bicarbonate

waters), to up to 37 µg per 100 mg in the region M = 550 to 1100 mg L^{-1} (when sodic waters become dominant). With further evolution (M > 1000 mg L^{-1}), the rate of uranium accumulation in solution decreases again (9 µg per 100 mg), due to the sustained loss of uranium to secondary phases. These secondary phases are found, in the simulation, to be from the pitchblende ("black") oxide group, containing hexavalent and tetravalent uranium in ratios between 1:2 and 1:3. The dominant secondary uranium minerals are found to be, initially, uraninite UO_2, α-U_4O_9, β-U_4O_9 and, as the mineralisation exceeds 1000 mg L^{-1}, α-U_3O_7, β-U_3O_7 and coffinite. In our simulated conditions (temperature = 10°C, P_{tot} = 1 MPa, $P_{CO2} = 10^{-2.5}$ atm., Eh = +50 mV, uranium content in rocks = 5 ppm), secondary uranium mineral formation commences at aqueous uranium concentrations of 100 µg L^{-1}.

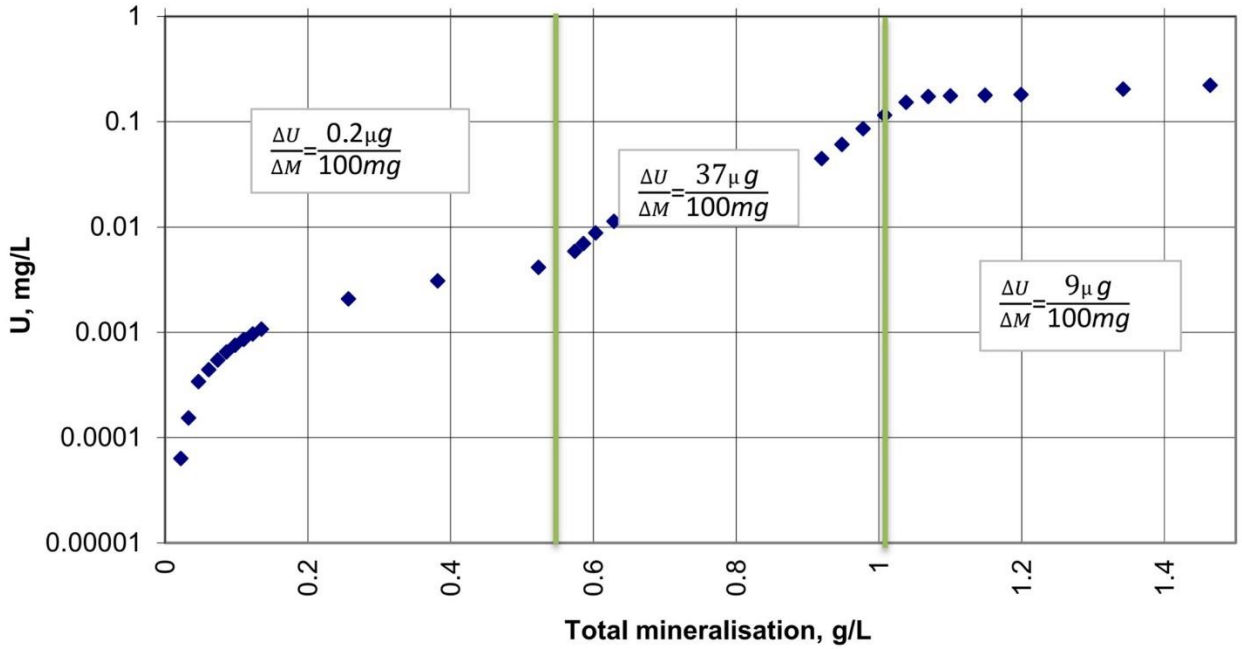

Figure 5. Dynamics of uranium accumulation in the simulated groundwater-granitoid system (temperature = 10°C, P_{tot} =1 MPa, $P_{CO2} = 10^{-2.5}$ atm., Eh = +50 mV, initial uranium content in rocks = 5 ppm).

Figure 6 shows the dependence of aqueous concentrations of uranium on the uranium content of the rocks. It is conceivable that this graphic actually has the potential to be used as a "nomogram" (i.e. an inverse model), to estimate the parent rock uranium content from the mineralisation and uranium content of the groundwater.

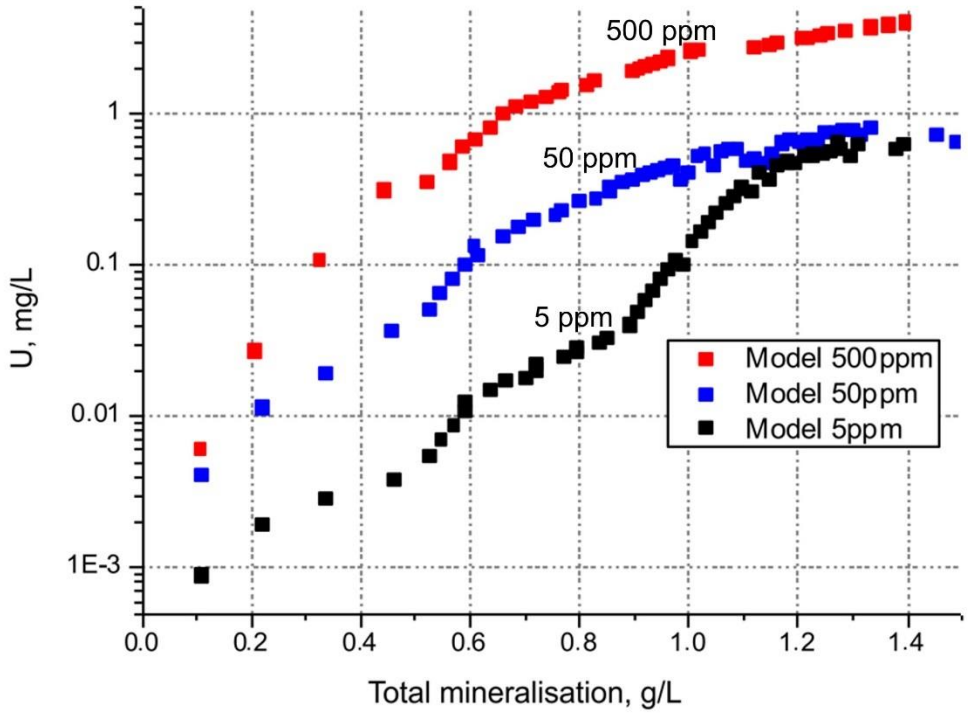

Figure 6. Accumulation of uranium in the aqueous phase in the simulated groundwater-granitoid system, for various parent rock uranium contents (temperature = 10°C, P_{tot} =1 MPa, $P_{CO2} = 10^{-2.5}$ atm., Eh = +50 mV, uranium content in rocks = 5 to 500 ppm).

3.2 Sensitivity of results to host rock uranium content and Eh

Modest alterations to the model parameterisation (e.g. uranium content of original rock, Eh of the solution) do not lead to fundamental changes in the pattern of uranium accumulation in the aqueous phase described above, although, together with pH, they do affect the point at which formation of secondary minerals occurs and thus the aqueous concentrations of U that are achieved. The formation of secondary uranium minerals seems to coincide with the formation of sodic (sodium bicarbonate) waters, albeit from solutions with somewhat different hydrochemical compositions and uranium concentrations (Table 3).

For example, with a parent rock uranium content of 5 ppm U, the formation of secondary minerals commences at a water mineralisation (*M*) around of around 930 mg L^{-1} when Eh = +5 mV and at about 1000 mg L^{-1} when Eh = +50 mV. Thus, with decreasing Eh (more reducing conditions), uranium encounters saturation thresholds at an earlier stage of hydrochemical evolution (lower mineralisation and pH).

Table 3. Impact of varying the initial rock uranium content and Eh on the onset of formation of secondary uranium minerals (temperature = 10°C, P_{tot} =1 MPa, $P_{CO2} = 10^{-2.5}$ atm.)

Concentration of uranium in primary rock, ppm	Eh of solution (mV)	Characteristic water chemistry at the onset of uranium secondary mineral formation		
		pH	Mineralisation *M* (mg L^{-1})	U at onset of secondary mineral formation, (µg L^{-1})
5	+5	7.4	>930	43
5	+50	7.42	>1000	100
5	+100	ne	ne	ne
500	+5	6.96	>110	0.2
500	+50	7.2	>340	356
500	+100	ne	ne	ne

ne = not attained in the modelled interval

With a parent rock uranium content of 50 ppm U, the pattern of evolution is not qualitatively different, but secondary uranium minerals begin to precipitate at a much earlier stage of evolution; when Eh = +5 mV, precipitation begins in the first modelling step at *M* = c. 110 mg L^{-1}, when aqueous uranium concentrations are less than 1 µg L^{-1}. With a somewhat higher Eh of c. +50 mV secondary uranium minerals begin to form at *M* = 340 g L^{-1}.

Under more oxidising conditions (Eh = +100 mV), the model does not predict the formation of secondary uranium minerals within the modelled mineralisation interval (i.e. at $M < 10$ g L^{-1}).

Based on these results we can conclude that the formation of secondary uranium minerals is very Eh sensitive, and therefore that the redox conditions suitable for the mobilisation and subsequent formation of secondary uranium deposits are likely to be relatively uncommon and specific to zones of steep redox gradients (geochemical "barriers"). The hydrochemical evolution patterns identified in the simulations are consistent with the findings of previous studies such as those of (Lisitsin 1967, 1971).

3.3 Sensitivity of results to assumptions about CO_2 conditions

To examine the influence of CO_2 conditions on uranium mobilisation, the simulations were repeated under the same conditions (10°C, 1 MPa total pressure), and CO_2 partial pressures

were varied within the range $10^{-2.5}$ to $10^{-0.5}$ atmospheres (Figure 7). The system was open with respect to CO_2. The partial pressure of $10^{-0.5}$ atm. is rather high to be realistic for soil gas or recharge water, but 10^{-2} or $10^{-1.5}$ atm is a realistic figure for CO_2 concentrations found in soil gas and new recharge water, even in relatively unproductive soil systems (such as in Norway, Banks & Frengstad, 2006).

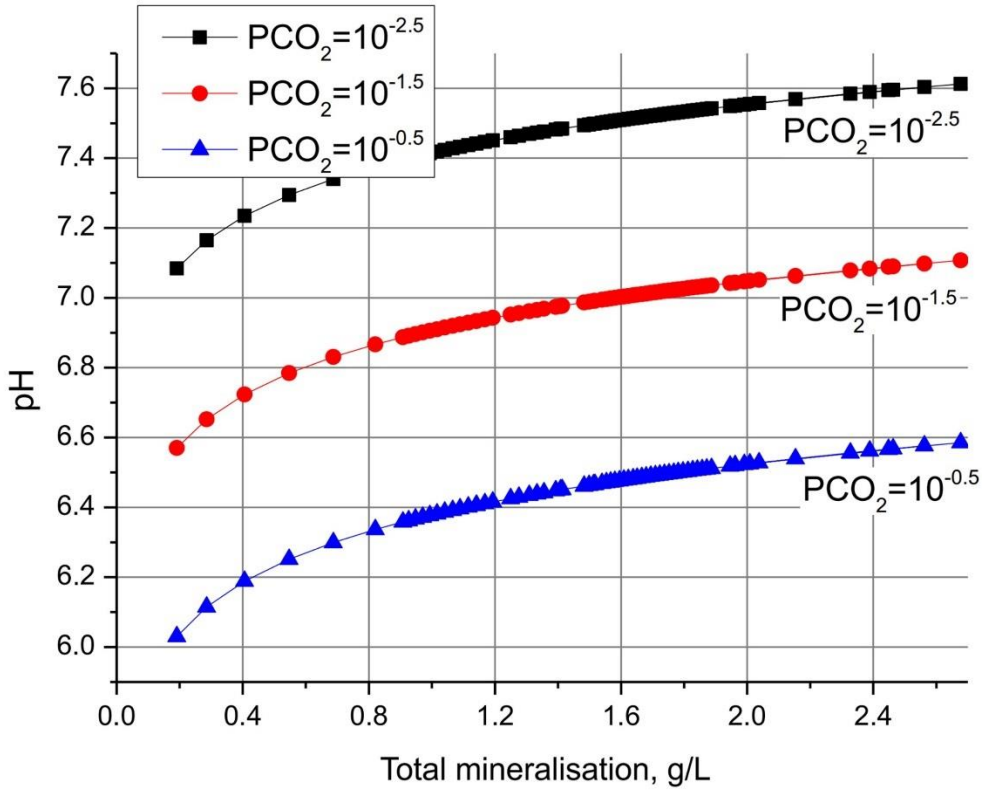

Figure 7. The evolution of the pH of the aqueous phase simulated in the groundwater-granitoid system, as a function of total water mineralisation (temperature = 10°C, P_{tot} = 1 MPa, P_{CO2} = $10^{-0.5}$, $10^{-1.5}$ and $10^{-2.5}$ atm., Eh = +50 mV, uranium content in rocks = 5 ppm)

Figure 7 illustrates that the pH value is controlled by the available partial pressure of CO_2. The curves have similar shape in each case and the pH increases by 0.5 units in the mineralisation interval 150 to 1500 mg L^{-1}. One order of magnitude increase in the CO_2 partial pressure typically results in 0.5 units of pH decrease. In reality, the CO_2 content experienced by the water-mineral system will depend on temperature, biological activity in the soil zone, diffusion processes, gas-phase/dissolved-phase dynamics (and also the degree of closure of the system: here it is assumed that the system is open with respect to CO_2). Furthermore, it has been shown that the mobility of uranium is directly affected by complexation with elements of the carbon-dioxide-carbonate system (Barsukov & Borisov, 2003). Table 4 summarizes the impact of varying P_{CO2} on the formation of secondary uranium minerals

Table 4. Impact of varying the CO_2 partial pressure on the onset of formation of secondary uranium minerals (temperature = 10°C, P_{tot} = 1 MPa, Eh = +50mV, rock uranium content = 5 ppm).

P_{CO2} (atm.)	pH and mineralisation *M* of solution at commencement of secondary uranium mineral formation (mg L^{-1})		Uranium minerals formed
	pH	*M*	
$10^{-2.5}$	7.42	1000	Uraninite, "Black" U oxides
$10^{-1.5}$	7.01	1770	"Black" U oxides
$10^{-0.5}$	6.61	3100	Uraninite, "Black" U oxides

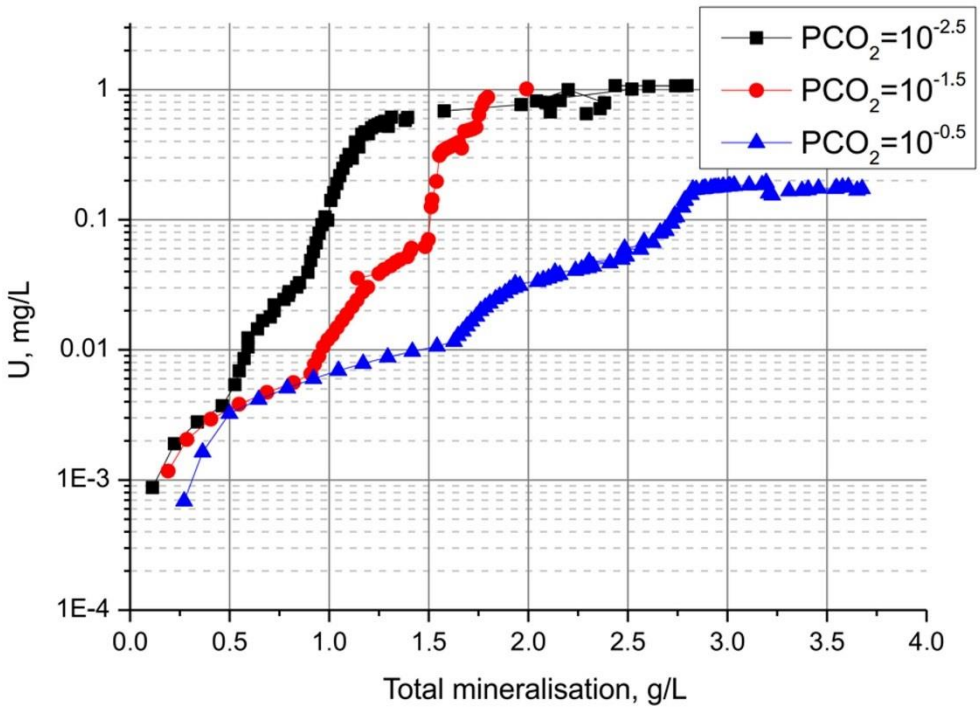

Figure 8. Dependence of aqueous uranium concentrations in groundwater on mineralisation for varying CO_2 partial pressure (from $10^{-2.5}$ to $10^{-0.5}$ atm.), for temperature = 10°C, P_{tot} = 1 MPa and content of uranium in primary mineral assemblage = 5 ppm.

It can be seen from Table 4 that the evolution of the behaviour of uranium in the system is heavily dependent on the CO_2 conditions. Further detail can be found in Figure 8, which demonstrates that, for a P_{CO2} of $10^{-1.5}$ to $10^{-2.5}$ atm. (which range corresponds well with natural groundwater systems), it is possible to achieve up to just over 1 mg L^{-1} uranium in the simulated groundwater system with 5 ppm uranium in the primary mineral assemblage. This corresponds very well with the Norwegian groundwater data, where maximum concentrations in exactly this range are observed (Frengstad & Banks 2014). The lower the P_{CO2}, the "earlier" (i.e. the lower the total mineralisation) secondary uranium mineral precipitation commences and the

earlier an apparent "saturation ceiling" appears. However, in the mineralisation interval 0 to c. 600 mg L^{-1}, characteristic for the Siberian and Norwegian study areas considered below (Section 5), uranium concentrations typically do not exceed 10 µg L^{-1}.

4. Discussion: Field Comparison and Verification

In order to "reality-check" the results of the simulations, they have been compared with groundwater quality data collected from two research areas (Figure 9):

- Groundwaters from the Alta-Sayan orogenic belt, south-western Siberia, Russian Federation

- Groundwater from Norwegian crystalline bedrock aquifers (ranging in age from Precambrian basement, through rocks of the Caledonian orogenic belt, to late Palaeozoic igneous rocks of the Oslo Rift).

Within these regions, granitoids (often rather radioactive) are widespread, as are occurrences of various types of uranium mineralisation (Lindahl 1983, Dahlkamp 2009). The groundwater hydrochemistries of these two study areas have been widely investigated and documented from both practical (water resources) and theoretical viewpoints (Dutova *et al.* 2006, Shvartsev *et al.* 2007, Balobanenko *et al.* 2016 for the Russian area; Banks *et al.* 1998, Frengstad *et al.* 2000, 2001, Banks & Frengstad 2006, Frengstad & Banks 2007, 2008, 2014 for Norway).

Figure 9. Overview map showing the locations of the study areas: 1 – Norway; 2 – south-western Siberia (including the Altai-Sayan mountain belt).

4.1 Groundwaters of the Altai-Sayan orogenic belt

The Altai-Sayan orogenic belt comprises a series of eroded mountain ranges (the Western and Eastern Sayan, the Altai, the Kuznetsk Alatau, etc.), separated by intermontane basins (Tuva, Rybinsk, Kuznetsk, Minusinsk etc. – see Figure 10).

The orogenic belts comprise intensely metamorphosed sedimentary and volcanic rocks of Archean, Proterozoic, Lower and Middle Palaeozoic ages, in highly compressed, sometimes overturned, fold structures, cut by numerous faults and intruded by igneous rocks of various compositions. The intermontane basins comprise gently folded Palaeozoic and Mesozoic rocks, partially overlain by Cenozoic sediments. Truly mountainous relief is found only in the very cores of the orogenic belts, the bulk of which comprise terrain with a relief of 1000-2000 m above sea level (asl). Lower hilly relief characterises the foothills of the Altai, Sayan, Kuznetsk Alatau and the Salair structure and the Kolyvan'-Tomsk folded zone. The intermontane basins

398 are characterised by low hills or flat land, with altitudes of between 125-150 m asl (Rybinsk
399 basin) to 1000-1200 m asl (Altai basin).
400
401 The ecology and landscape of the area are closely related to relief. Subalpine meadows and
402 mountain tundra occupy the highlands and areas of middle relief (around 20% of the region).
403 Forest taiga dominates the middle-low altitude mountain areas and the foothills, while sub-
404 taiga forest occupies the peripheries of the intermontane basins. Steppe and forest-steppe
405 landscape is characteristic of the intermontane basins and also significant parts of the foothills
406 and even middle elevations. The mountainous areas are rather wet and a high modulus of
407 groundwater run-off is estimated (3 - 6 L s^{-1} km^{-2}), whereas that in the drier intermontane basins
408 is much lower at around (0.1 – 0.5 L s^{-1} km^{-2}).
409
410 The hydrogeology of the region is complex. The rocks are consolidated to varying degrees and
411 fracture flow of various types (including some karstic) is dominant. Groundwater circulation
412 is believed to be within an exogenous fractured zone of 50-80 m thickness, although in discrete
413 fracture structures significant circulation may reach 100 m or more. Artesian conditions occur
414 in the intermontane basins. The general direction of regional groundwater flow is from the
415 mountains towards the artesian intermontane basins or towards the Western Siberian artesian
416 megabasin. The main areas of groundwater discharge are the local river valley systems.
417

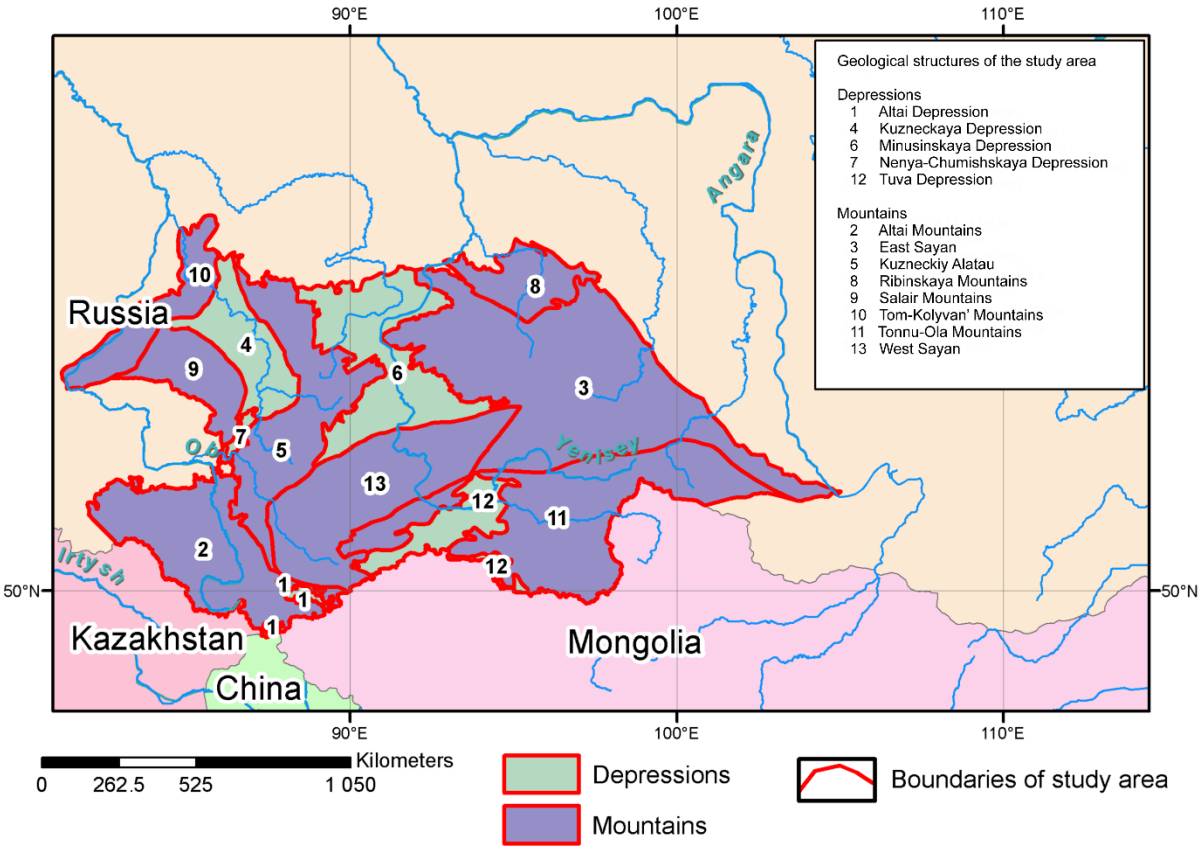

Figure 10. Structural elements of the Altai-Sayan region of Western Siberia (for location, see Figure 9).

An interplay of tectonic, climatic and lithological conditions, together with precipitation characteristics and altitudinal landscape zonation, conspires to give the groundwaters their characteristic hydrochemistry (Table 5). Typical groundwaters of the fractured aquifers of the mountain-meadow-taiga terrain of the Sayan, Altai and Kuznetsk Alatau mountains have a typical mineralisation of c. 340-400 mg L^{-1}, are of sodium-magnesium-calcium bicarbonate composition, and are neutral to slightly alkaline. In the taiga and forest-steppe terrain of the Salair and Kolyvan'-Tomsk structures, groundwaters tend to be more highly-mineralised, circumneutral to slightly alkaline, bicarbonate waters, mainly dominated by magnesium-calcium in their cation content. In these regions, the major ion chemistry does not predominantly depend on rock type and is controlled by more universal reactions governing water-rock interaction (see Frengstad & Banks 2007, Shvartsev *et al.* 2007). More deeply-circulating groundwaters, sometimes associated with fault zones, are characterised by a greater residence time and hydrogeochemical "maturity": sodium-bicarbonate composition is characteristic, as are mineralisations of up to 1500 mg L^{-1}, or more.

Table 5. Average chemical compositions of groundwater from the zone of shallow groundwater circulation (hypergene zone) of the Altai-Sayan orogenic belt and adjacent structures of the West Siberian plate (mg L^{-1}, except for U in µg L^{-1}; compiled from Shvartsev *et al.* 2007)

Components	Mountains					Intermontane basins					Adjacent structures of West-Siberian plate
	Altai	Sayan	Kuznetsk Alatau	Salair	Tomsk-Kolyvan'	Altai	Tuva	Kuznetsk	Rybinsk	Minusinsk	
pH	7.4	6.9	7.3	7.5	7.5	7.6	8.1	7.5	7.6	7.8	7.5
HCO_3^-	218	201	225	404	497	246	367	469	402	348	392
SO_4^{2-}	20	21	19	5	13	60	53	55	67	213	105
Cl^-	17	26	14	9	16	44	29	32	19	108	71
Ca^{2+}	48	37	56	93	76	40	60	93	85	72	43
Na^+	21	24	18	20	43	72	52	59	98	155	147
Mg^{2+}	15	23	17	16	37	15	33	34	32	40	25
SiO_2	11	8	14	19	15	16	6	19	7	12	16
Sum	352	340	400	574	705	530	594	758	752	983	795
U	0.88	1.12	0.77	0.57	1.05	5.00	-	2.4	-	8.15	3.1
number of samples	930	1309	3319	1796	2468	44	71	94	300	130	360

In the steppe terrain of the intermontane basins and adjacent structures of the West Siberian Plain, the majority of groundwaters are of bicarbonate type, with mineralisation not exceeding c. 1000 mg L^{-1}. However, more brackish waters of varying ionic composition can also be found ($Na\text{-}HCO_3$ $Ca\text{-}Na\text{-}Cl\text{-}HCO_3$, $Na\text{-}Ca\text{-}SO_4\text{-}HCO_3$, $Ca\text{-}Na\text{-}Cl\text{-}SO_4\text{-}HCO_3$ and even $Na\text{-}SO_4$ or, Na-Cl), in part due to the presence of evaporite minerals within the sedimentary rock sequences. In general, these lower altitude groundwaters enjoy a longer residence time and greater degree of water-rock interaction, whilst evaporative concentration of salts is also believed to also play an important role (Parnachev *et al.* 1999, Banks *et al.* 2004).

The uranium concentrations in the studied waters of the region range from a few hundredths to a few hundred µg L^{-1}. In the waters of the folded mountain belt, the uranium concentrations are modest at typically several tenths of µg L^{-1} (Table 4). Concentrations are somewhat higher in the lower altitude waters and in the zones of know uranium mineralisation (Gornii Altai, Sayan, Kolyvan'-Tomsk). The highest uranium concentrations (tens or, in exceptional cases, hundreds

of μg L^{-1}) are associated with water-bearing fault structures in the orogenic belts, associated with uranium or sulphide mineralisation. In these structures, as well as a generally high metals content in the rocks, the oxidation of sulphide minerals and dissolution of hydrothermally altered mineral assemblages may also play a role in uranium mobilisation. This interpretation is supported by the fact that the groundwaters in such zones generally have a high total mineralisation and elevated calcium and sulphate concentrations, as well as high uranium concentrations.

The groundwaters of the intermontane basins of the region, derived from subsurface run-off from the surrounding mountains and influenced by evaporative concentration in a shallow oxidising steppe environment (Parnachev *et al.*1999, Banks *et al.* 2004), are characterised by elevated uranium concentrations. Typical uranium concentrations are in the several μg L^{-1} range, with even higher concentrations (tens to hundreds μg L^{-1}) in some water seepages and springs. In general, higher uranium concentrations correlate with elevated total mineralisation of waters.

Deeper groundwaters (presumed more reducing geochemical environment) are characterized by substantially (one order of magnitude) lower concentrations of uranium, although a positive correlation between uranium and total mineralization is still observed.

Actual uranium concentrations are plotted against total groundwater mineralisation on several of the simulated evolution curves in Figure 11.

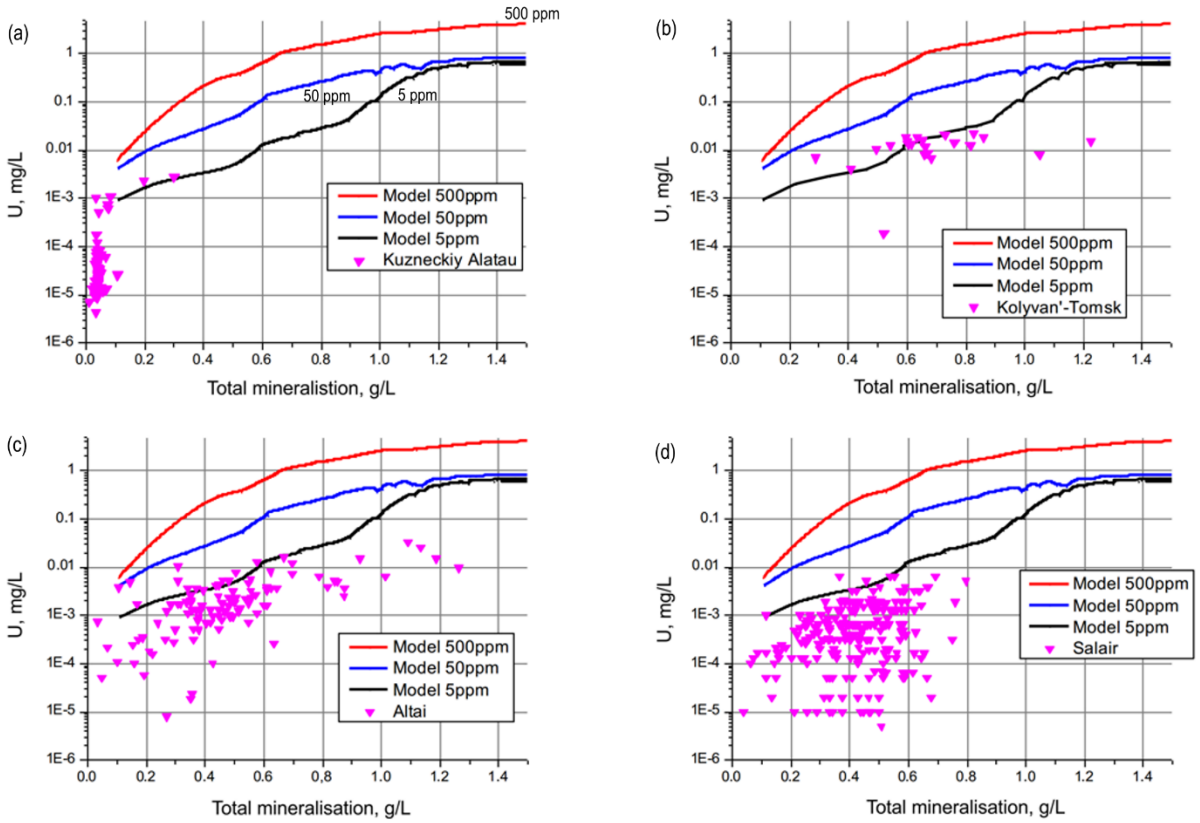

Figure 11. Dissolved uranium versus total groundwater mineralisation in the Altai-Sayan region, compared with the simulated groundwater-granitoid system (temperature = 10°C, P_{tot} = 1 MPa, $P_{CO2} = 10^{-2.5}$ atm., Eh = +50 mV, uranium content in rocks from 5 to 500 ppm). (a) Kuznetsk Alatau (granitoids), (b) Kolyvan'-Tomsk (granitoids), (c) Altai (various rocks), (d) Salair (various rocks).

Analysis of these data indicates that the general magnitude of uranium concentrations predicted by the simulations is close to those observed in the field study area. In both the simulated and real data, there is a general increase in uranium concentration with total mineralisation. The distribution of real uranium concentrations tends to bear closest resemblance to the models where the primary rock uranium content is around 5 ppm. Groundwaters from the granitoids of Kuznetsk Alatau match the simulated evolutionary trend for uranium up to a mineralisation of around 300 mg L^{-1} and are characterized by rather low uranium concentrations. The distribution of uranium in groundwaters of the granitoids of the Kolyvan'-Tomsk folded zone corresponds to a mineralisation range from 300 to 1200 mg L^{-1}. The low groundwater uranium concentrations from Salair correspond with the low uranium content of the rocks (< 5 ppm), while the large range of uranium concentration in Altai also reflects the large variation in rock types and their radioelement contents.

Significant mineral-forming concentrations of aqueous uranium (such as are obtained from the simulations – Table 3) are, for the most part, not observed in the zones of regional fracturing. The exception appears to be waters derived from specific local fault zones. Such uranium-rich waters may be able to participate in hydrogene formation of low temperature uranium mineralisation or uranium ore genesis in the marginal parts of intrusions within volcanoclastic formations.

One can speculate that groundwater from the mountain belts, with a relatively modest uranium content, flows in the subsurface towards the artesian structures of the intermontane basins or towards the West Siberian artesian megabasin. Such long flow pathways under oxidizing conditions, coupled with evapoconcentrative steppe processes, tend to lead to progressive elevation in uranium concentrations (Figure 10). Such waters, on encountering reducing geochemical "barriers" may be able to form uranium deposits from aqueous solution, which typically leads to a drop in dissolved uranium concentration of around two orders of magnitude. As far as current knowledge allows, it appears that in this region, hydrogene uranium deposits form within platform cover sediments and with palaeo-depression structures at oxidation/-reduction barriers. Moreover, rich ore deposits, of industrial relevance, occur at ancient structural-stratigraphic unconformities (Kislyakov & Shchetochkin 2000, Domarenko *et al.* 2010).

4.2 Crystalline bedrock groundwaters from Norway

Between 1996 and 1998, the Geological Survey of Norway sampled 1604 groundwaters from Norway's crystalline rock aquifers, many (but not all) of which comprise granitoids or granitic gneisses (Banks *et al.* 1998, Frengstad *et al.* 2000). As regards uranium content, Killeen & Heier (1975a,b) report arithmetic mean uranium contents of 5.7, 9.9, 5.5 and 4.7 ppm for the Flå, Iddefjord, Bohus and Drammen granites of the Oslo area, respectively, but lower mean U contents (0.7 to 2.3 ppm) for the Farsund granites of southern Norway. Regrettably, neither mineralisation (*M*), nor sodium accumulation can be used as indicators of groundwater hydrochemical maturity in Norway's coastal environment, as sodium and chloride mineralisation can be due to the influence of marine salts, as well as to, for example, aluminosilicate hydrolysis. In the discussion, below, three proxy indicators of hydrochemical maturity have been utilised:

(i) total alkalinity (in most cases, this simply represents the water's bicarbonate content)
(ii) the lithologically derived sodium (Na*) content, having been corrected for marine salts on the basis of chloride, where Na*=Na-Cl×(10556/18980) in mg L^{-1}, based on a typical marine sodium concentration of 10556 mg L^{-1} and chloride 18980 mg L^{-1} (Lenntech 2016).
(iii) the Na*/Ca meq ratio = Na* × 20.04 / (Ca × 22.99)

In the 1996-98 study, 476 of the Norwegian waters were analysed for uranium by ICP-MS techniques (Frengstad *et al.* 2000, 2001). The median uranium concentration of these water was 2.5 µg L^{-1}, while the maximum was 750 µg L^{-1}. These magnitudes support the observation (Figure 8) that simulated uranium concentrations in relatively unevolved groundwaters (M < 600 mg L^{-1}) are generally < 10 µg L^{-1}, although concentrations of up to just over 1 mg L^{-1} can be observed at higher degrees of hydrochemical evolution (or greater host rock U contents). Indeed, uranium concentration up to a maximum of 2 mg L^{-1} have been observed in other Norwegian studies (Frengstad & Banks 2014).

In the 1996-98 (N=476) study, a large number of the waters exhibited pH values around 8.0 (60% of the waters had pH in the range 7.74 to 8.22). This clustering effect means that it is very difficult to observe pH-related trends on standard x-y diagrams of covariance (Figure 12c,d). It appeared that, in many waters, the pH was buffered around 8.0 to 8.2 and it was hypothesised that this represented precipitation of calcite from the waters and the transition to sodium bicarbonate-dominated waters (Banks & Frengstad 2006). To circumvent the data clustering effect, Frengstad *et al.* (2001) ranked the data according to pH and divided it into 5 equal quintiles (Figure 12a,b).

It will be seen (Figure 12b) that Na* tends to increase slightly with increasing pH (judging from the numbers of zero or negative calculated Na* for each pH subgroup), but with a major increase in the last pH subgroup (pH > 8.2) indicating that, at high pH, sodium has become the dominant cation. Uranium also initially increases with increasing pH, up to a pH of around 8. Following this, U concentrations decline slightly again, although there is very large variance in each pH subgroup (which may reflect both lithological and kinetic factors). This decrease at elevated pH values could be considered to represent depletion due to precipitation as secondary minerals, as predicted by the HydroGeo simulations. As noted above, the maximum U concentrations of a few hundred µg L^{-1} agree rather well with the HydroGeo simulations.

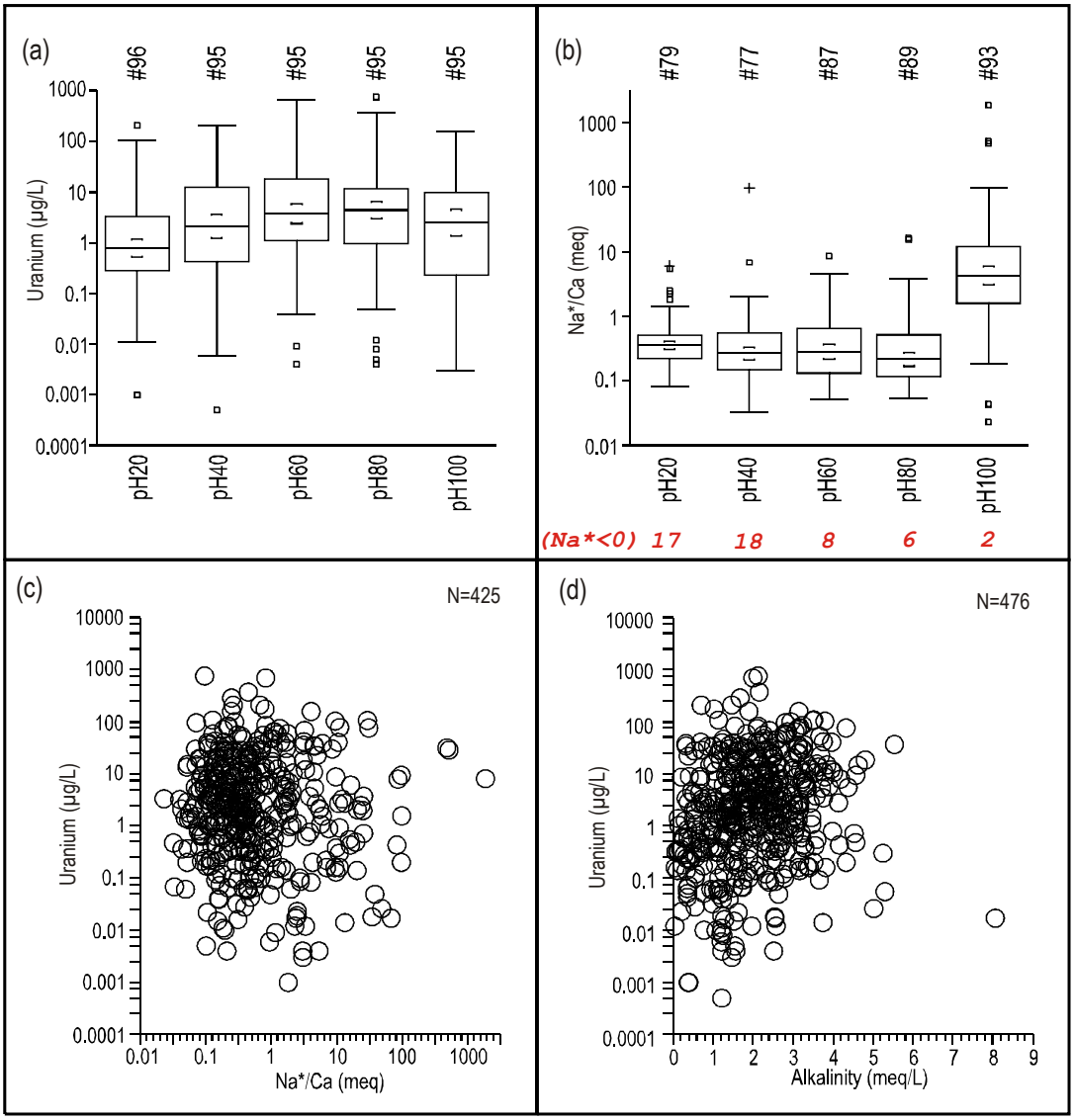

Figure 12. The relationship between dissolved uranium, total alkalinity and the meq ratio between lithologically derived sodium (Na*) and calcium in 476 Norwegian crystalline bedrock groundwaters (the dataset reported by Frengstad *et al.* 2000, 2001). Na* = lithological sodium (Na*=Na-Cl×(10556/18980), based on typical marine sodium concentration of 10556 mg L^{-1} and chloride 18980 mg L^{-1} - Lenntech 2016). Where Na* is calculated as <0, data for Na*/Ca are omitted from the logarithmic scaled plots (b) and (c). The red figures at the base of the boxes in Figure 12(b) denote the number of data points omitted due to Na* being calculated as a (near-zero) negative value. The subsets pH20 to pH100 represent ranked quintiles of the dataset according to pH: pH20 represents pH from 6.18 to 7.73; pH40 represents 7.74 to 8.01; pH60 represents 8.01 to 8.13; pH80 represents 8.14 to 8.22; pH100 represents 8.22 to 9.58. # denotes numbers of data in each subset.

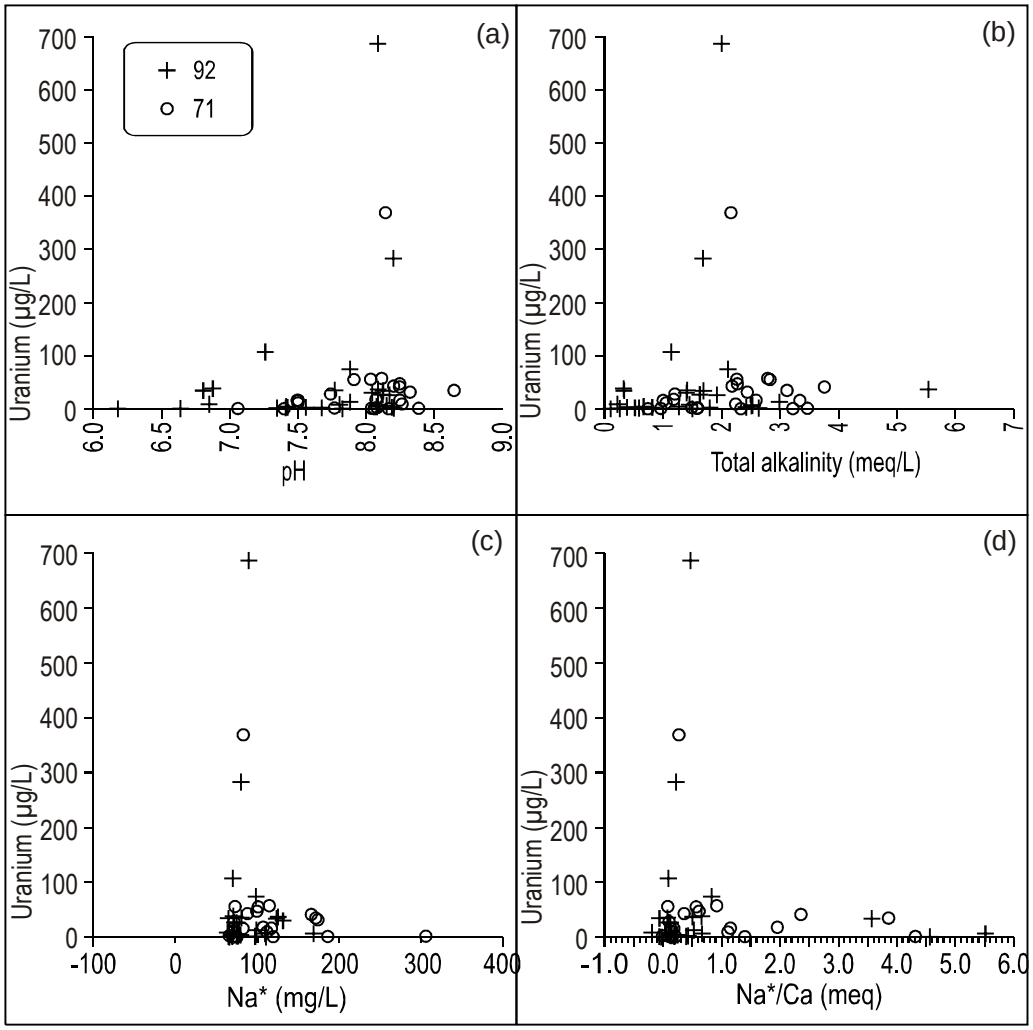

Figure 13. The relationship between dissolved uranium, total alkalinity and the meq ratio between lithologically derived sodium (Na*) and calcium in two subsets of the Norwegian crystalline bedrock groundwaters shown in Figure 12 (the 1996-98 dataset reported by Frengstad *et al.* 2000, 2001). Na* = lithological sodium (Na*=Na-Cl×(10556/18980), based on typical marine sodium concentration of 10556 mg L^{-1} and chloride 18980 mg L^{-1} (Lenntech 2016). Group 71 = groundwaters from Norwegian Caledonian granite to tonalite (N = 24); Group 92 = groundwaters from Norwegian autochthonous Precambrian granite to tonalite (N= 29)

In order to remove the variability in mineralogy and rock uranium content in the 1996-98 (N=476) data set, two lithological subgroups of the Norwegian data have been selected: Group 71 (N=24), representing granitoids of the Caledonian orogenic belt and Group 92 (N=29), representing "autochthonous" Precambrian granites (Figure 13). In a lithological analysis (Frengstad *et al.* 2000), these two granitic groundwater subgroups were demonstrated to exhibit generally higher uranium concentrations than other lithological subsets, presumably reflecting the higher uranium contents of the granites. It will be noted that the generally highest uranium

concentrations in the granitoid data are observed around pH 8, lithologically-derived sodium concentrations of c. 100 mg L^{-1} (which agrees quite well with the modelling findings in Section 3), alkalinities of around 2 meq L^{-1} and Na*/Ca meq ratios of <1 (i.e. before the stage of sodium bicarbonate waters is reached).

Thus, while the Norwegian data exhibits significant support for the modelled scenarios, in terms of the general pattern of uranium accumulation, the typical maximum concentrations and the approximate concentrations of lithologically-derived sodium at which maximum uranium accumulation rates occur, there are also some significant differences:

- the Norwegian waters exhibit much higher pH values than predicted by the HydroGeo simulation. Banks & Frengstad (2006) have hypothesised that the groundwater systems cannot be fully "open" with respect to CO_2, and must experience some degree of "closure" in order to explain the high pH of the Norwegian waters.
- with pH increasing beyond 8, the Norwegian waters exhibit a modest trend to decreasing uranium concentrations. This is not observed in the HydroGeo model; while the rate of accumulation decreases at elevated pH due to uranium mineral precipitation, dissolved concentrations do not. This may also be related to the fact that, because the HydroGeo simulation is "open" with respect to CO_2, pH values do not approach or exceed pH 8. It may also be hypothesised that the highest pH Norwegian waters tend to be more deeper and reducing in nature.
- in the Norwegian field data, maximum uranium concentrations are observed before the water achieves an alkaline sodium composition.

All of this leads us to speculate that dissolved uranium concentrations in groundwater are controlled by three master variables:

(i) the total uranium content in the parent mineral assemblage (see Table 3)
(ii) the Eh (see Table 3)
(iii) the pH, which is in turn affected by CO_2 conditions

and maybe not by the transition to sodic waters in itself. In many silicate-dominated groundwater systems, the transition to sodic waters tends to occur when the system is buffered at a relatively high pH by secondary calcite precipitation (which releases protons to the water).

$$Ca^{++} + HCO_3^- = CaCO_3 + H^+ \quad (1)$$

Thus, the approximate coincidence of the transition to sodic waters with an optimum pH for uranium mobilisation may be largely fortuitous.

5. Summary and Conclusions

Modelling of water-rock interaction using the software package "HydroGeo" has confirmed a number of known or suspected geochemical principles regarding the accumulation of uranium in shallow groundwaters in granitoid aquifers:

(1) In the simulated oxidising environment, uranium occurs predominantly in solution in its hexavalent state.
(2) Increasing the host rock uranium content generally tends to increase the aqueous uranium concentration.
(3) Increasing Eh (at least within the range +5 to +100 mV) also tends to increase uranium mobilisation in the aqueous phase.

The simulations have also allowed the following hypotheses to be formulated:

(4) In rocks with a uranium content of 5 to 50 ppm in the primary mineral assemblage, it is possible to accumulate concentrations of uranium in the aqueous phase that result in precipitation of secondary uranium minerals.
(5) At a partial CO_2 pressure of $10^{-2.5}$ atm., the rate of accumulation of uranium in the aqueous phase seems to reach a maximum in the transitional domain between calcium-sodium and sodium bicarbonate water, as calcite approaches saturation. The highest uranium concentrations in oxidising environments are predicted to occur in alkaline sodium bicarbonate water types, where calcium has been depleted by calcium saturation.

(6) Uranium accumulation in solution is hindered in hydrochemically mature waters by saturation with respect to, and the thermodynamic likelihood of precipitation of "black" pitchblende-type mixed hexavalent-tetravalent uranium oxides.

(7) For moderate mineralisations and P_{CO2} between $10^{-1.5}$ and $10^{-2.5}$ atm., aqueous concentrations of uranium of up to 10 µg L^{-1} are typical in the simulations for rocks with 5-50 ppm U. This observation corresponds very well with the median concentration of 2.5 µg L^{-1} observed in N=476 Norwegian groundwaters (Frengstad et al. 2000). At higher groundwater mineralisations (i.e. greater degrees of water-rock interaction), simulations suggest that concentrations of just over 1 mg L^{-1} can evolve, which again corresponds well with the maximum concentration of 750 µg L^{-1} observed in N=476 Norwegian groundwaters (Frengstad et al. 2000) and the maximum observed Norwegian concentration of 2 mg L^{-1} (Frengstad & Banks 2014).

(8) The accumulation of uranium in the aqueous phase is strongly dependent on the partial pressures of CO_2, which in turn influence the evolution of pH. In systems open to CO_2, higher pH values are observed at lower P_{CO2} and saturation with respect to secondary uranium minerals is achieved at an earlier stage of hydrochemical evolution (lower mineralisation) than at higher values of P_{CO2}. Moreover, uranium appears to accumulate more rapidly in solution, relative to the rate of accumulation of total aqueous mineralisation, at lower P_{CO2}.

(9) The simulations where P_{CO2} has been varied strongly suggest that there are several key influences on uranium accumulation in water and that it is impossible to draw general rules regarding the stage at which uranium becomes saturated with respect to secondary minerals (i.e. specific pH, mineralisation or hydrogeochemical facies transition).

These observations can be tested against existing data sets for groundwater quality from granitoid rocks and may also be of use in prospecting for secondary uranium deposits.

Acknowledgements

The research described in this paper was carried out at Tomsk Polytechnic University within the framework of the Tomsk Polytechnic University Competitiveness Enhancement Program grant.

694 **References**

695 Alekseev, V.A., Riyzhenko, B.H., Shvartsev, S.L., Dutova, E.M. et al. *[Алексеев В.А.,*
696 *Рыженко Б.Н., Шварцев С.Л., Дутова Е.М. и др.]* (2005) Геологическая эволюция и
697 самоорганизация системы вода-порода в 5 томах. Том 1: Система вода - порода в
698 земной коре: взаимодействие, кинетика, равновесие, моделирование *[Geochemical*
699 *evolution and self-organisation of water rock systems (5 volumes): Volume 1: The system*
700 *water - rock in the earth's crust: interaction, kinetics, equilibrium, modeling - in Russian]*.
701 СО РАН, Novosibirsk, 244 pp

702 Allison, J.D.. Brown, D.S., Novo-Gradac, K.J., 1991. MINTEQA2/PRODEFA2, a
703 geochemical assessment model for environmental systems: Version 3.0 User's Manual.
704 United States Environmental Protection Agency report EPA/600/3-91/021. Athens,
705 Georgia, USA. 107 pp.

706 Anderson, G.M., 2009. Thermodynamics of Natural Systems (2nd edition). Cambridge
707 University Press. 648 pp.

708 Ariunbileg, S., Gaskova, O., Vladimirov, A., Battushig, A., Moroz, E., 2016. Spatial
709 distribution of uranium and metalloids in groundwater near sandstone-type uranium
710 deposits, Southern Mongolia. Geochemical Journal 50, 393-401. doi:
711 10.2343/geochemj.2.0434.

712 Arthur, R.C., 2001. A comment on the internal consistency of thermodynamic databases
713 supporting repository safety assessments. SKI Report 01-46. Statens kärnkraftinspektion
714 (Swedish Nuclear Power Inspectorate), Stockholm, Sweden.

715 Bain, J.G., Mayer, K.U., Blowes, D.W., Frind, E.O., Molson, J.W.H., Kahnt, R., Jenk, U.,
716 2001. Modelling the closure-related geochemical evolution of groundwater at a former
717 uranium mine. Journal of Contaminant Hydrology 52, 109-135. doi: 10.1016/S0169-
718 7722(01)00155-3.

719 Babin, G.A., Yuryev, A.A., Bichkov, A.I. Dubskii, V.S., Shigrev, A.F. *[Г.А. Бабин, А.А.*
720 *Юрьев, А.И. Бычков, В.С. Дубский, А.Ф. Щигрев]*, 2007. State Geological Map of the
721 Russian Federation Scale 1:1,000,000, Geological Map Sheet N-45 (Novokuznetsk),
722 ВСЕГЕИ, Ministry of Natural Resources of the Russian Federation, Moscow.
723 http://www.vsegei.ru/ru/info/pub_ggk1000-3/Altae-Sayanskaya/n-45.php (accessed
724 20.04.16).

725 Ball, J.W., Nordstrom, D.K., 2001. User's manual for WATEQ4F, with revised

726 thermodynamic database and test cases for calculating speciation of major, trace and redox
727 elements in natural waters. United States Geological Survey Open File Report 91-183,
728 originally published 1991, revised and reprinted 2001. Manlo Park, California, USA. 188
729 pp.

730 Balobanenko, A.A., L'gotin, V., Dutova, E.M., Pokrovsky, D.S., Nikitenkov, A.N., Raduk I.V.,
731 2016. Geochemical groundwater peculiarities of Paleogene sediments in S-E Western Siberia
732 artesian basin. IOP Conference Series: Earth and Environmental Science 43(1), art. no.
733 012030. doi: 10.1088/1755-1315/43/1/012030.

734 Banks, D., Frengstad, B., Midtgård, Aa.K., Krog, J.R., Strand, T., 1998. The chemistry of
735 Norwegian groundwaters: I. The distribution of radon, major and minor elements in 1604
736 crystalline bedrock groundwaters. Science of the Total Environment 222, 71-91. doi:
737 10.1016/S0048-9697(98)00291-5.

738 Banks, D., Parnachev, V.P., Frengstad, B., Holden, W., Karnachuk, O.V., Vedernikov A.A.,
739 2004. The evolution of alkaline, saline ground- and surface waters in the southern Siberian
740 steppes. *Applied Geochemistry* 19, 1905-1926. doi: 10.1016/j.apgeochem.2004.05.009.

741 Banks, D., Frengstad, B., 2006. Evolution of groundwater chemical composition by plagioclase
742 hydrolysis in Norwegian anorthosites. Geochimica et Cosmochimica Acta 70, 1337-1355.
743 doi: 10.1016/j.gca.2005.11.025.

744 Banks, D., Parnachev, V.P., Frengstad, B., Karnachuk, O.V., 2008. Hydrogeochemical data
745 report: the sampling of selected locations in the Republic of Khakassia, Kuznetsk Alatau
746 oblast' and Kemerovo oblast', Southern Siberia, Russian Federation. Norges geologiske
747 undersøkelse (Geological Survey of Norway) report 2008.013.
748 http://www.ngu.no/upload/Publikasjoner/Rapporter/2008/2008_013.pdf (accessed
749 20.04.16).

750 Banks, D., Parnachev, V.P., Karnachuk, O.V., Arkhipov, A.L., Gundersen, P., Davis, J., 2011.
751 Hydrogeochemical data report: the sampling of selected localities in Kemerovo oblast' and
752 Tomsk oblast', Siberia, Russian Federation. Norges geologiske undersøkelse (Geological
753 Survey of Norway) report 2011.054.
754 http://www.ngu.no/upload/Publikasjoner/Rapporter/2011/2011_054.pdf (accessed
755 20.04.16).

756 Barnett, M.O., Jardine, P.M., Brooks, S.C., Selim, H.M., 2000. Adsorption and transport of
757 uranium (VI) in subsurface media. Soil Science Society of America Journal 64, 908-917.

758 doi: 10.2136/sssaj2000.643908x.

759 Barsukov, V.L, Borisov, M.V. *[Барсуков В.Л., Борисов М.В.]*, 2003. Модели растворения
760 урана в природных водах разного состава *[Models of uranium dissolution in natural*
761 *waters of varying composition - in Russian]*. Геохимия 1, 43-69.

762 Berman, R.G., 1988. Internally-consistent thermodynamic data for minerals in the system
763 Na_2O-K_2O-CaO-MgO-FeO-Fe_2O_3-Al_2O_3-SiO_2-TiO_2-H_2O-CO_2. Journal of Petrology 29,
764 445-522. doi: 10.1093/petrology/29.2.445.

765 Bukaty, M.B. *[Букаты М.Б.]*, 2002. Разработка программного обеспечения для решения
766 гидрогеологических задач *[Development of software for solving hydrogeological*
767 *problems - in Russian]*. *In* "Geology prospecting and exploration of mineral resources of
768 Siberia", Известия Томского политехнического университета 305(6), 348-365.

769 Bukaty, M.B. *[Букаты М.Б.]*, 2005a. Рекламно-техническое описание программного
770 комплекса HydroGeo. *[Advertising and technical description of the software package*
771 *HydroGeo - in Russian]* All-Russian Scientific and Technical Information Centre
772 (ВНТИЦ), Registration of Algorithms and Programmes No. 50200500605. ВНТИЦ,
773 Moscow, 7 pp.

774 Bukaty, M.B. *[Букаты М.Б.]*, 2005b. Проблемы качества численных моделей системы
775 вода-порода *[Numerical models of water-rock systems: quality problems - in Russian]*.
776 Chapter 6.7 in: Shvartsev, S.L. (Ed.) Геологическая эволюция и самоорганизация
777 системы вода-порода в 5 томах. Том 1: Система вода-порода в земной коре.
778 взаимодествие, кинетика, равновесие, моделирование *[Geochemical evolution and*
779 *self-organisation of water rock systems (5 volumes): Volume 1: Water-rock systems in the*
780 *earth's crust: interaction, kinetics, equilibrium, modelling – in Russian]*. СО РАН,
781 Novosibirsk: 243-332.

782 Bukaty, M.B. *[Букаты М.Б.]*, 2008. Численные методы моделирования геомиграции
783 радионуклидов: Методические указания к выполнению лабораторных работ для
784 студентов направления магистерской подготовки "урановая геология" *[Numerical*
785 *methods for modelling the geomigration of radionuclides: Methodological guidelines for*
786 *laboratory work for Masters students in uranium geology - in Russian]*. Tomsk
787 Polytechnical University document УДК 550.46, Tomsk, 73 pp.

788 Bukaty, M.B., Dutova, E.M., Balobanenko, A.A., Kuzevanov, K.I. *[Букаты М.Б., Дутова*
789 *Е.М., Балобаненко А.А., Кузеванов К.И.]*, 2010. Моделирование геохимического

поведения урана в подземных водах юго-восточной окраины Западно-Сибирского бассейна *[Modelling the geochemical behaviour of uranium in groundwaters of the south-eastern region of the Western Siberian basin - in Russian]*. Разведка и охрана недр. 11, 49–54.

Chudnenko, K.V. *[Чудненко К.В.]*, 2010. Термодинамическое моделирование в геохимии: теория, алгоритмы, программное обеспечение, приложения *[Thermodynamic modelling in geochemistry: Theory, algorithms, software, applications - in Russian]*. Russian Academy of Science, Siberian Division, A.P. Vinogradov Institute of Geochemistry, Novosibirsk, 247 pp. ISBN: 978-5-904682-18-7.

Cleverley, J.S., Bastrakov, E.N., 2005. K2GWB: Utility for generating thermodynamic data files for The Geochemist's Workbench® at 0–1000 °C and 1–5000 bar from UT2K and the UNITHERM database. Computers and Geosciences 31, 756–767. doi: 10.1016/j.cageo.2005.01.007.

Dahlkamp, F.J., 2009. Yenisey Region. Chapter 10.3 in: Uranium Deposits of the World: Asia. Springer, 493 pp.

Domarenko, V.A., Chernev, E.M., Sobolev, I.S *[Домаренко, В.А., Чернев, Е.М., Соболев, И.С.]*, 2010. Возможности обнаружения уранового оруденения гидрогенного типа на востоке Западно-Сибирской плиты *[Possibility of hydrogenious type uranium ore discovery in the West Siberia platform – in Russian].* Разведка и охрана недр. 11, 24-32.

Dong, W., Brooks, S.C., 2006. Determination of the formation constants of ternary complexes of uranyl and carbonate with alkaline earth metals (Mg^{2+}, Ca^{2+}, Sr^{2+} and Ba^{2+}) using anion exchange method. Environmental Science and Technology 40, 4689-4695. doi: 10.1021/es0606327.

Dutova, E.M., Bukaty, M.B., Nevol'ko, A.I., Pokrovsky, D.S., Shvartsev, S.L. *[Дутова Е.М., Букаты М.Б., Неволько А.И., Покровский Д.С., Шварцев С.Л.]*, 2006. Гидрогенное концентрирование золота в аллювиальных россыпях Егорьевского района (Салаир) *[Hydrogenic concentration of gold in alluvial placers of the Egor'evsk area (Salair) - in Russian]*. Геология и Геофизика 47(3), 364-376.

Dutova, E.M., Nikitenkov, A.N. *[Е.М. Дутова, Никитенков А.Н.]*, 2010. Физико-химическое моделирование поведения урана в системе «вода - гранитоиды» *[Physico-chemical modelling of the behaviour of uranium in the granitoid-water system - in Russian]*. Вестник Томского государственного университета 330, 202-207.

Dutova, E., Vologdina, I., Pokrovsky, D., Nalivaiko, N., Kuzevanov, K., Pokrovsky, V., 2016. Hydrogenous mineral neoformations in Tomsk water intake facility from underground sources. IOP Conference Series: Earth and Environmental Science 33(1), art. no. 012017. doi: 10.1088/1755-1315/33/1/012017.

Frengstad, B., Midtgård Skrede, Aa., K., Banks, D., Krog, J.R., Siewers, U., 2000. The chemistry of Norwegian groundwaters. III. The distribution of trace elements in 476 crystalline bedrock groundwaters, as analysed by ICP-MS techniques. Science of the Total Environment 246, 21-40. doi: 10.1016/S0048-9697(99)00413-1.

Frengstad, B., Banks, D., Siewers, U., 2001. The chemistry of Norwegian groundwaters: IV. The pH-dependence of element concentrations in crystalline bedrock groundwaters. Science of the Total Environment 277, 101-117. doi: 10.1016/S0048-9697(00)00867-6.

Frengstad, B., Banks, D., 2007. Universal controls on the evolution of groundwater chemistry in crystalline bedrock: The evidence from empirical and theoretical studies. In: Krásný, J., Sharp, J.M. (Eds.), Groundwater in Fractured Rocks. Taylor & Francis/Balkema, pp. 275-289.

Frengstad, B., Banks, D., 2008. The natural inorganic chemical quality of crystalline bedrock groundwaters of Norway. Chapter 20 in: Edmunds, W.M., Shand, P. (Eds.), Natural Groundwater Quality. Blackwell, Oxford, pp. 421-440. ISBN: 9781405156752. doi: 10.1002/9781444300345.ch20.

Frengstad, B.S., Banks, D., 2014. Uranium distribution in groundwater from fractured crystalline aquifers in Norway. In: Sharp, J.M. (Ed.), Fractured Rock Hydrogeology. International Association of Hydrogeologists Selected Papers 20, pp. 257-276. CRC Press/ Taylor & Francis, London. ISBN 9781138001596. doi: 10.1201/b17016-17.

Gaskova, O.L., Shironosova, G.P., Kabannik, V.G., Bukaty, M.B., 2009. Thermodynamic model for sorption of bivalent heavy metals on calcite in natural-technogenic environments. Russian Geology and Geophysics Volume 50, №2, pp. 87-95.

Grenthe, I., Fuger, J., Konings, R.J.M., Lemire, R.J., Muller, A.B., Nguyen-Trung, C., Wanner, H. (1992). *Chemical Thermodynamics of Uranium*. Elsevier, New York, 715 pp.

Harvie, C.E., Moller, N., Weare, J.H., 1984. The prediction of mineral solubilities in natural waters: the Na-K-Mg-Ca-H-Cl-SO4-OH-HCO3-CO3-CO2-H2O system to high ionic strength at 25℃. Geochimica et Cosmochimica Acta 48, 723-751. doi: 10.1016/0016-

7037(84)90098-X.

Helgeson, H.C., Delany, J.M., Nesbitt, H.W., Bird, D.K., 1978. Summary and critique of the thermodynamic properties of rock-forming minerals. American Journal of Science 278-A, 1-229.

Johnson, J.W.; Oelkers, E.H.; Helgeson, H.C., 1992. SUPCRT92: A software package for calculating the standard molal thermodynamic properties of minerals, gases, aqueous species, and reactions from 1 to 5000 bar and 0 to 1000°C. Computers and Geosciences 18, 899-947. doi: 10.1016/0098-3004(92)90029-Q.

Kharaka, Y.K., Gunter, W.D., Aggarwal, P.K., Perkins, E.H., De Braal, J.D., 1988. SOLMINEQ.88: A computer program for geochemical modeling of water-rock interactions. United States Geological Survey Water Resources Investigation Report 88-4227. Menlo Park, California, USA. 420 pp.

Killeen, P.G., Heier, K.S., 1975a. A uranium and thorium enriched province of the Fennoscandian shield in southern Norway. Geochimica et Cosmochimica Acta 39, 1515-1524. doi: 10.1016/0016-7037(75)90153-2.

Killeen, P.G., Heier, K.S., 1975b. Trend surface analysis of Th, U, and K, and heat production in three related granitic plutons, Farsund area, south Norway. Chemical Geology 15, 163-176. doi: 10.1016/0009-2541(75)90017-0.

Kislyakov, Ya.M., Shchetochkin, V.N., 2000. Hydrogenic ore-forming systems. Geology of Ore Deposits 42, 369-396.

Kondratyeva, I.A., Lisitsin, A.K., Komarova, G.V. *[Кондратьева И.А., Лисицин, А.К., Комарова, Г.В.]*, 1980. Типы гидрогенных месторождений урана *[Types of hydrogenic uranium deposits - in Russian]*. In: Perel'man, A.I. (Ed.) Гидрогенные месторождения урана. Основы теории образования *[Hydrogene uranium ores – fundamentals of the theory of formation]*. Atomizdat; Moscow, pp. 135-138.

Kondratyeva, I.A., Nesterova, M.V. *[Кондратьева И.А., Нестерова М.В.]*, 2002. Инфильтрационные урановые месторождения в мезозойских речных палеодолинах Западной Сибири *[Uranium infiltration ores in the Mesozoic riverine palaeovalleys of Western Siberia - in Russian]*. In: Gavrilin, G.I. (Ed.), Уран на рубеже веков: природные ресурсы, производство, потребление *[Uranium at the turn of the century: natural resources, production, consumption]*. ВИМСа, Moscow, pp. 144-158.

884 Korobeinikov, A.F., Domarenko, V.A., Vladimirova, E.V., Rikhvanov, L.P., 1983. Gold in the
885 rocks of postorogenic gabbro-syenite-granite intrusives at Kuznetskii Alatau. Izvestiya
886 Akademii Nauk SSSR, Seriya Geologicheskaya 12, 107-119.

887 Krainov, S.R., Riyzhenko, B.N., Shvets, V.M. *[Крайнов С.Р., Рыженко Б.Н., Швец В.М.]*,
888 2004. Геохимия подземных вод. Теоретические, прикладные и экологические
889 аспекты *[Groundwater Geochemistry. Theoretical, Applied and Ecologiucal Aspects - in*
890 *Russian*]. Наука, Moscow, 677 pp.

891 Lietsch, C., Hoth, N., Kassahun, A., 2014. Thermodynamic characterization of dissolved
892 uranium species in flooded uranium nines and tailing management facilities. In: Sui, W.,
893 Sun, Y., Wang, C. (Eds.), An interdisciplinary response to mine water challenges.
894 Proceedings of the 12th IMWA Congress. China University of Mining and Technology
895 Press, Xuzhou. 137-141.

896 Lenntech, 2016. Major ion composition of seawater (mg/L). Lenntech water treatment
897 solutions. http://www.lenntech.com/composition-seawater.htm (accessed 20.04.16).

898 Lindahl, I., 1983. Classification of uranium mineralisation in Norway. Norges geologiske
899 undersøkelse Bulletin 380, 125-142.

900 Lisitsin, A.K. *[Лисицин, А.К.]*, 1967. Метод определения Eh-pH химического равновесия
901 водного раствора с горными породами и минералами *[A method of Eh-pH*
902 *determination for chemical equilibrium of aqueous solution with rocks and minerals -in*
903 *Russian]*. Геохимия 8, 994-1000.

904 Lisitsin, A.K., 1971. Ratio of the redox equilibria of uranium and iron in stratiform aquifers.
905 International Geology Review 13, 744-751. doi: 10.1080/00206817109475493.

906 Lisitsin, A.K. *[Лисицин, А.К.]*, 1996. Гидрогеохимическая модель инфильтрационной
907 рудообразующей системы *[Hydrogeochemical model of infiltrational ore-forming system*
908 *– in Russian]*. Геохимия 3, 294-304.

909 Parkhurst, D.L., Appelo, C.A.J., 1999. User's guide to PHREEQC (Version 2) - A computer
910 program for speciation, batch-reaction, one-dimensional transport, and inverse
911 geochemical calculations. U.S. Geological Survey Water Resources Investigations Report
912 99-4259, 310 pp.

913 Parnachev, V.P., Banks, D., Berezovsky, A.Y., Garbe-Schönberg, D., 1999. Hydrochemical
914 evolution of Na-SO_4-Cl groundwaters in a cold, semi-arid region of southern Siberia.

915 Hydrogeology Journal 7, 546-560. doi: 10.1007/s100400050228.

916 Reimann, C., Banks, D., 2004. Setting action levels for drinking water: Are we protecting our
917 health or our economy (or our backs!)? Science of the Total Environment 332, 13-21. doi:
918 10.1016/j.scitotenv.2004.04.007.

919 Runde, W., 2000. The chemical interactions of actinides in the environment. Los Alamos
920 Science 26, 392-411.

921 Shvarov, Y.V., Bastrakov, E.N., 1999. HCh: a software package for geochemical equilibrium
922 modelling (user's guide). Australian Geological Survey Organization, Record 1999/25, 61
923 pp.

924 Shvartsev, S.L., Dutova, E.M., 2001. Hydrochemistry and mobilization of gold in the
925 hypergenesis zone (Kuznetsk Alatau, Russia). *Geology of Ore Deposits* 43(3), 224-233.

926 Shvartsev, S.L., Riyzhenko, B.H., Alekseev, V.A., Dutova, E.M., Kondratyeva, I.A., Kopilova,
927 Y.G., Lepokurova, O.E. *[Шварцев С.Л., Рыженко Б.Н., Алексеев В.А., Дутова Е.М.,*
928 *Кондратьева И.А., Копылова Ю.Г., Лепокурова О.Е.]*, 2007. Геологическая эволюция
929 и самоорганизация системы вода-порода в 5 томах. Том 2: Система вода-порода в
930 условиях зоны гипергенеза *[Geochemical evolution and self-organisation of water rock*
931 *systems (5 volumes): Volume 2: Water-rock systems in the hypergene zone - in Russian]*.
932 СО РАН, Novosibirsk, Russia, 389 pp.

933 Stewart, B.D., 2008. The dominating influence of calcium on the biogeochemical fate of
934 uranium. PhD dissertation, Dept. of Civil and Environmental Engineering, Stanford
935 University, USA. May 2008. Website:
936 http://soils.stanford.edu/theses/brandythesisjun2222.pdf, accessed 29th June 2017.

937 Voroshilov V., Savinova O., Ananev Yu., Abramova R., 2014. Anomaly geochemical fields in
938 Siberian hydrothermal gold deposits. IOP Conference Series: Earth and Environmental
939 Science 21(1), art. no. 012009. doi: 10.1088/1755-1315/21/1/012009.

940 WHO, 2012. Uranium in drinking-water (Background document for development of "WHO
941 Guidelines for Drinking-water Quality"). Document WHO/SDE/WSH/03.04/118/Rev/1,
942 World Health Organisation, Geneva, 21 pp.
943 http://www.who.int/water_sanitation_health/publications/2012/background_uranium.pdf
944 (accessed 04.05.17).

945